Dynamics near homoclinic bifurcations of three-dimensional dissipative diffeomorphisms

ANTONIO PUMARIÑO
Departamento de Matemáticas, Universidad de Oviedo
Calvo Sotelo s/n, 33.007 Oviedo, Spain
e-mail: apv@pinon.ccu.uniovi.es

JOAN CARLES TATJER
Departament de Matemàtica Aplicada i Anàlisi,
Universitat de Barcelona
Gran Vía, 585, 08.007 Barcelona, Spain
e-mail: jcarles@maia.ub.es

Abstract

We explore the complicated dynamics arising in a neighbourhood of a homoclinic point associated to a homoclinic bifurcation of a two-parameter family of three-dimensional dissipative diffeomorphisms. We place ourselves in the case in which the unstable manifold of the periodic saddle involved in the homoclinic bifurcation has dimension two. Besides proving the existence of strange attractors with two positive Lyapounov exponents for the associated limit return map, we also select a curve in the space of parameters in order to numerically detect the presence of possible new families of one-dimensional and two-dimensional strange attractors. The end of this curve of parameters corresponds to a return map which is conjugate to a "bidimensional tent map".

1 Introduction

From the pioneer work of Poincaré [18] it is well understood that, for a dynamical system, the presence of homoclinic orbits implies a very intricate geometrical structure in the respective phase space. Roughly speaking, a homoclinic orbit springs when an intersection between the stable and the unstable manifolds of a periodic point takes place. One of the most interesting problems posed during the last century was the one directed to describe what happens in a family of dynamical systems when a first homoclinic orbit is created. This first homoclinic orbit corresponds to a tangential connection between the above mentioned invariant manifolds and the phenomenon of creation or destruction of homoclinic orbits is known as "unfolding of homoclinic tangencies".

During the last three or four decades an ambitious program is being carried out in order to understand the rich dynamics associated to the unfolding of homoclinic tangencies for parameter families of two-dimensional diffeomorphisms. From the initial works of S. Newhouse, J. Palis and F. Takens to the present days a great effort was made to analytically prove the existence of complicated dynamical objects (infinitely many sinks, strange attractors,...) in the two-dimensional scenario. Most of those results are based on the existence of limit return maps defined in a neighbourhood of the homoclinic orbit for values of the parameter close enough to that one giving rise to the first homoclinic tangency, see [15], [16], [23]. The advantage to work with these limit return maps is not only that they are essentially defined in a lower-dimensional setting (i.e., in the two-dimensional framework the core of the dynamics of the limit return maps is an interval), but also that we have an explicit expression for them (being this expression valid for generic families of two-dimensional diffeomorphisms exhibiting homoclinic tangencies unfolding generically).

We are going to deal with the unfolding of homoclinic tangencies in a three-dimensional scenario for two-parameter families of diffeomorphisms. Hence, in order to describe the notion of limit return map we recover from [24] a definition not depending on the dimension of the manifold in which the diffeomorphisms are defined:

Definition 1 *Let $\{f_a\}_{a\in V}$ be a smooth family of diffeomorphisms in some m-dimensional manifold M, depending on a parameter $a \in V \subset \mathbb{R}^k$, V being an open subset. Suppose that for $a = a_0$ there exists a homoclinic orbit O_0 of some dissipative fixed point p_0 of f_{a_0}. We say that the family $\{f_a\}_{a\in V}$ has a family of **limit return maps** associated to the homoclinic orbit O_0, in the C^l topology, if there exists a point q of the homoclinic orbit and a natural number N, such that for any positive integer $n \geq N$ there exist reparametrizations $a = M_n(\widetilde{a})$ of the a variable and $\widetilde{a}$-dependent coordinate transformations $x = \Psi_{n,\widetilde{a}}(\widetilde{x})$ satisfying the following properties:*

1.- For each compact set K in the $(\widetilde{a}, \widetilde{x})$ space the images of K under the maps

$$(\widetilde{a}, \widetilde{x}) \rightarrow (M_n(\widetilde{a}), \Psi_{n,\widetilde{a}}(\widetilde{x}))$$

converge, for $n \rightarrow \infty$, in the $(\widetilde{a}, \widetilde{x})$ space, to (a_0, q).

2.- The domains of the maps

$$(\widetilde{a}, \widetilde{x}) \rightarrow \left(\widetilde{a}, \left(\Psi^{-1}_{n,\widetilde{a}} \circ f^n_{M_n(\widetilde{a})} \circ \Psi_{n,\widetilde{a}}\right)\right)$$

converge, for $n \rightarrow \infty$, to $\mathbb{R}^{m+k}$, and the maps converge, in the C^l topology, to some map of the form

$$(\widetilde{a}, \widetilde{x}) \rightarrow \left(\widetilde{a}, \widetilde{f}_{\widetilde{a}}(\widetilde{x})\right).$$

In this case, we say that $\left\{\widetilde{f}_{\widetilde{a}}\right\}_{\widetilde{a}\in\mathbb{R}^k}$ is a family of limit return maps associated to the homoclinic orbit O_0.

With respect to the above definition, we recall that a fixed point p of a diffeomorphism f defined in a manifold of dimension m is said to be dissipative if $|\lambda_1 \cdots \lambda_m| < 1$, where $\lambda_1, \ldots, \lambda_m$ are the eigenvalues of $Df(p)$.

In a few words, the existence of a family $\left\{\widetilde{f}_{\widetilde{a}}\right\}_{\widetilde{a}\in\mathbb{R}^k}$ of limit return maps means that, up to a change of coordinates, the dynamics (in a neighbourhood of some homoclinic point) of a sufficiently large power of f_a looks like the dynamics of some $\widetilde{f}_{\widetilde{a}}$. As we said before, the main point here is to obtain the explicit expression of a family of limit return maps, being this expression valid for generic situations: Generic families of diffeomorphisms $\{f_a\}_{a\in V}$ having homoclinic tangencies unfolding generically.

For generic one-parameter families of diffeomorphisms on surfaces unfolding a homoclinic tangency, i.e., when $k = 1$ and $m = 2$, it can be shown, see [15] and [16], that the family of "bidimensional" return maps $\left\{\widetilde{f}_{\widetilde{a}}\right\}_{\widetilde{a}\in\mathbb{R}}$ is given by $\widetilde{f}_{\widetilde{a}}(\widetilde{x}) = (1 - \widetilde{a}\widetilde{x}_1^2, 0)$, $\widetilde{x} = (\widetilde{x}_1, \widetilde{x}_2)$. Therefore, these limit return maps essentially behaves as the one-dimensional logistic family $Q_a(x) = 1 - ax^2$.

This result was used by Mora and Viana, see [15], to prove that for each one of the above generic one-parameter families of diffeomorphisms on surfaces unfolding homoclinic tangencies the following property holds: They exhibit strange attractors (or repellors) with positive probability in the parameter space. Before going on, let us recall the definition of strange attractor:

Definition 2 *An **attractor** for a transformation f defined in a manifold M is a compact, f-invariant and transitive set A whose stable set*

$$W^s(A) = \{z \in M : d(f^n(z), A) \to 0 \ \text{as}\ n \to \infty\}$$

*has nonempty interior. An attractor is said to be **strange** if it contains a dense orbit $\{f^n(z_1) : n \geq 0\}$ displaying exponential growth of the derivative: There exists some constant $c > 0$ such that, for every $n \geq 0$,*

$$\|Df^n(z_1)\| \geq e^{cn}.$$

The results proved in [15] are strongly based in the fact that the logistic family $Q_a(x) = 1 - ax^2$ has strange attractors with positive probability, see [1], [2] and [9]. Hence, even in the two-dimensional setting, it is essential to study the dynamics of the limit return maps in order to describe the dynamics arising in the unfolding of homoclinic tangencies.

This was also the route for describing the dynamical properties for families unfolding homoclinic tangencies in some special higher-dimensional scenarios: For generic one-parameter families of diffeomorphisms (i.e., $k = 1$) defined in a manifold of arbitrary dimension m, a family of limit return maps can be also constructed when $\dim(W^u(p_0)) = 1$ and p_0 is sectionally dissipative: The eigenvalues of $Df_{a_0}(p_0)$ satisfy $|\lambda_1| \leq ... \leq |\lambda_{m-1}| < 1 < |\lambda_m|$ and $|\lambda_{m-1}\lambda_m| < 1$. Moreover, these limit return maps also behave as the one-dimensional logistic family $Q_a(x) = 1 - ax^2$.

Therefore the next step seems to be to deal with the unfoldings of homoclinic tangencies of diffeomorphisms defined in manifolds of dimension greater than two but without the assumption of sectional dissipation.

We will study the dynamics associated to the unfolding of homoclinic tangencies for certain two-parameter families ($k = 2$) of three-dimensional diffeomorphisms ($m = 3$)

which are dissipative but not sectionally dissipative: In the sectionally dissipative case, there already exist results concerning the coexistence of infinitely many sinks, see Palis and Viana [17], and strange attractors, see Viana [25].

In the not sectionally dissipative case we will also extensively use limit return maps (which are, once again, noninvertible maps) defined in some neighbourhood of the homoclinic orbit. Hence, we will start Section 2 by making an overview on the known results about the existence of limit return maps for the case in which $k = 2$, $m = 3$, the eigenvalues of the dissipative saddle are real and the assumption of sectional dissipation is not fulfilled. Let us denote by (a_0, b_0) the value of the parameter for which there exists a homoclinic tangency between the invariant manifolds of a saddle fixed point p_0 with real eigenvalues.

Depending on the behaviour of the eigenvalues λ_1, λ_2 and λ_3 of $Df_{a_0,b_0}(p_0)$ and on the dimension of the invariant manifolds of p_0, we will obtain three different families of limit return maps associated to the respective homoclinic orbit. As in the lower-dimensional setting (i.e., when $m = 2$), it will be enough to study these limit maps in a $(m-1)$-dimensional scenario. Hence, we are going to study two-parameter families of endomorphisms defined on $\mathbb{R}^2$. Since we are specially interested in topologically two-dimensional strange attractors we will focus our attention in the case in which the unstable manifold of p_0 has dimension two (we refer to this case as case B). In case B the respective family of endomorphisms is denoted by $T_{a,b}$, see (2). Section 2 is also devoted to find values of the parameter (a, b) for which the map $T_{a,b}$ has an invariant region (and therefore, an attractor). This set of parameters contains some piece of a curve G, see (4), ending at $(a, b) = (-4, -2)$. As in the lower-dimensional case (i.e., when $m = 2$) this final value of the parameter would be very relevant. We recall again that in the case in which $m = 2$ the limit return maps are given by

$$\widetilde{f}_{\widetilde{a}}(\widetilde{x}_1, \widetilde{x}_2) = \left(1 - \widetilde{a}\widetilde{x}_1^2, 0\right)$$

and the dynamical behaviour of these maps dramatically changes when the parameter cross the ("final") Misiurewicz value $\widetilde{a} = 2$. In fact, all the results concerning the existence of strange attractors, see [1], [9] and [15], have to be posed for sets of values of the parameter smaller than this final value.

Nevertheless, since the dynamical behaviour of $\widetilde{f}_2$ is extremely relevant to obtain the results in [1] and [9] (and even in [15]) we conclude Section 2 by studying the dynamical properties of our final transformation $T_{-4,-2}$.

Section 3 is devoted to show the richness of the one-dimensional and two-dimensional strange attractors for several values of (a, b) in the piece of the curve G for which we can guarantee the existence of an invariant domain for $T_{a,b}$.

A preliminary version of these results can be found in [21].

2 Return maps in the not sectionally dissipative case

In general, a one-parameter family of three-dimensional diffeomorphisms not satisfying the assumption of sectional dissipation does not have limit return maps. Therefore, we must work with two-parameter families of such diffeomorphisms and we must add certain extra assumption over the geometry of the homoclinic tangency. The existence of two-parameter families of limit return maps associated to these two-parameter families of three-dimensional diffeomorphisms in the not sectionally dissipative case has been recently proved in [24]. We refer the reader to [24] to get information about the definitions and the assumptions needed to prove the main result there, see Theorem 1. We only outline here those parts of Theorem 1 in [24] which we are going to explore:

Let us consider a two-parameter family $\{f_{a,b}\}_{a,b}$ of three-dimensional diffeomorphisms having a hyperbolic saddle fixed point p_0 for $(a,b)=(0,0)$ with real eigenvalues λ_1, λ_2 and λ_3 satisfying the following properties (we refer the reader to [24] for the definition of generalized homoclinic tangency and the statement of the linearization assumption):

1.- Either $|\lambda_1|<|\lambda_2|<1<|\lambda_3|$ and $|\lambda_1\lambda_3|<1$, $|\lambda_2\lambda_3|>1$ (case A) or $|\lambda_1|<1$, $|\lambda_3|>|\lambda_2|>1$ (case B). We remark that from this assumption the corresponding fixed point is never sectionally dissipative.

2.- The invariant manifolds of p_0 have a generalized homoclinic tangency which unfolds generically (we only remark here that in the set of two-parameter families of three-dimensional diffeomorphisms unfolding homoclinic tangencies those ones unfolding a **generalized** homoclinic tangency are generic).

3.- The family $\{f_{a,b}\}_{a,b}$ satisfies the linearization assumption (generic condition for families of diffeomorphisms having saddle fixed points).

Under the above three assumptions, Theorem 1 in [24] ensures that there exists a family of limit return maps $\left\{\widetilde{f}_{\widetilde{a},\widetilde{b}}\right\}$, $\left(\widetilde{a},\widetilde{b}\right)\in\mathbb{R}^2$, associated to the homoclinic orbit. Moreover, these limit return maps are given by:

$$\widetilde{f}_{\widetilde{a},\widetilde{b}}\left(\widetilde{x},\widetilde{y},\widetilde{z}\right)=\left(\widetilde{z},\widetilde{b}\widetilde{z},\widetilde{a}+\widetilde{y}+\widetilde{z}^2\right)\text{ or }\widetilde{f}_{\widetilde{a},\widetilde{b}}\left(\widetilde{x},\widetilde{y},\widetilde{z}\right)=\left(0,\widetilde{z},\widetilde{a}+\widetilde{b}\widetilde{y}+\widetilde{z}^2\right)$$

in case A and by:

$$\widetilde{f}_{\widetilde{a},\widetilde{b}}\left(\widetilde{x},\widetilde{y},\widetilde{z}\right)=\left(\widetilde{z},\widetilde{a}+\widetilde{b}\widetilde{y}+\widetilde{z}^2,\widetilde{y}\right)\tag{1}$$

in case B.

Let us remark that, although in case A there exist two possible families of limit return maps, only one of them can be applied depending on the geometry of the tangency, see [24] for details. Moreover, the map in case B appears as a rescaled map also in the cases of simple quadratic homoclinic tangencies of manifolds of saddle-focus fixed points (see [8]).

The second family of transformations in case A is equivalent to the family

$$\widetilde{H}_{\widetilde{a},\widetilde{b}}\left(\widetilde{x},\widetilde{y}\right)=\left(\widetilde{a}+\widetilde{x}^2+\widetilde{b}\widetilde{y},\widetilde{x}\right)$$

which is conjugate (just taking $X=\widetilde{x}$ and $Y=\widetilde{b}\widetilde{y}$) to the Hènon family

$$H_{\widetilde{a},\widetilde{b}}\left(X,Y\right)=\left(\widetilde{a}+X^2+Y,\widetilde{b}X\right),$$

except for the case in which $\widetilde{b}=0$.

The first family of endomorphisms in case A is conjugate to the second one in case A except for $\widetilde{b}=0$ (it is enough to take the change of coordinates $\widetilde{X}=\widetilde{b}\widetilde{x}-\widetilde{y}$, $\widetilde{Y}=\widetilde{b}^{-1}\widetilde{y}$, $\widetilde{Z}=\widetilde{z}$). When $\widetilde{b}=0$ the dynamics of both families of return maps in case A coincide, and they essentially behave as the dynamics of the unimodal family $\widetilde{Q}_{\widetilde{a}}\left(\widetilde{x}\right)=\widetilde{a}+\widetilde{x}^2$.

Hence, since we are specially interested in two-dimensional attractors we fix our attention in the family of return maps for the case in which the unstable manifold of the saddle fixed point involved in the homoclinic tangency has dimension two (case B), see (1). The case A has been extensively studied in [7].

2.1 Return maps for case B

Let us begin by pointing out that, for each $\left(\widetilde{a},\widetilde{b}\right)\in\mathbb{R}^2$, every point in $\mathbb{R}^3$ "falls" by one iteration of the map $\widetilde{f}_{\widetilde{a},\widetilde{b}}$, see (1), into the surface

$$C_{\widetilde{a},\widetilde{b}}=\left\{\left(\widetilde{x},\widetilde{y},\widetilde{z}\right):\widetilde{y}=\widetilde{a}+\widetilde{b}\widetilde{z}+\widetilde{x}^2\right\}.$$

Hence, $C_{\widetilde{a},\widetilde{b}}$ is invariant by $\widetilde{f}_{\widetilde{a},\widetilde{b}}$ and it is enough to study the dynamics of $\widetilde{f}_{\widetilde{a},\widetilde{b}}$ on $C_{\widetilde{a},\widetilde{b}}$. Therefore, the study of the initial family of three-dimensional transformations $\left\{f_{a,b}\right\}_{a,b}$ would start by working with two-dimensional endomorphisms. This fact is, as we say in the Introduction, a natural extension of the lower-dimensional case $m=2$, in which the core of the dynamics for the respective limit return maps is a one-dimensional set.

Using the parameterization of $C_{\widetilde{a},\widetilde{b}}$ given by $P\left(\widetilde{x},\widetilde{z}\right)=\left(\widetilde{x},\widetilde{a}+\widetilde{b}\widetilde{z}+\widetilde{x}^2,\widetilde{z}\right)$, in order to study the behaviour of $\widetilde{f}_{\widetilde{a},\widetilde{b}}$ on $C_{\widetilde{a},\widetilde{b}}$ it suffices to consider the family of bidimensional endomorphisms defined on $\mathbb{R}^2$ by

$$\left(P^{-1}\circ\widetilde{f}_{\widetilde{a},\widetilde{b}}\circ P\right)\left(\widetilde{x},\widetilde{z}\right)=\left(\widetilde{z},\widetilde{a}+\widetilde{b}\widetilde{z}+\widetilde{x}^2\right).$$

Let us take the change of coordinates $x=\widetilde{z}-\widetilde{b}\widetilde{x}$, $y=\widetilde{x}$ in order to write the above family of transformations in the following way

$$T_{a,b}\left(x,y\right)=\left(a+y^2,x+by\right),\tag{2}$$

where we have taken, in order to avoid tedious notation, $a=\widetilde{a}$ and $b=\widetilde{b}$.

Let us observe that (2) is a family of noninvertible maps, each one of them having two fixed points (whenever $(b-1)^2\geq 4a$) given by

$$P_{a,b}=\left((1-b)\frac{1-b+\sqrt{(b-1)^2-4a}}{2},\frac{1-b+\sqrt{(b-1)^2-4a}}{2}\right)$$

$$\widetilde{P}_{a,b}=\left((1-b)\frac{1-b-\sqrt{(b-1)^2-4a}}{2},\frac{1-b-\sqrt{(b-1)^2-4a}}{2}\right).\tag{3}$$

Since we look for attractors let us start by searching parameters for which we can guarantee the existence of invariant regions for $T_{a,b}$. The most simple situations arise by taking $b = 0$ because in this case $T_{a,0}(x, y) = (a + y^2, x)$ and $T^2_{a,0}(x, y) = (a + x^2, a + y^2)$. In particular, it follows that $T_{a,0}(R_a) = R_a$ for any $a \in [-2, -1]$, where $R_a = [a, a + a^2] \times [a, a + a^2]$. Furthermore, we prove the existence of bidimensional strange attractors (in a one-dimensional persistent way) for the family $T_{a,0}$ according to the following result:

Proposition 3 *For any $0 < c < \log 2$ there exists $a_0 > -2$ and a positive Lebesgue measure set E of values of the parameter a contained in $[-2, a_0]$ such that for any $a \in E$ there exists a dense orbit $\bigcup_{n\in\mathbb{N}} \left\{T^n_{a,0}(x_0, y_0)\right\}$ in R_a and a natural number n_0 such that*

$$\left\|DT^n_{a,0}(x_0, y_0)\,\mathbf{v}\right\| \geq \exp\left(\frac{cn}{2}\right)$$

for any unit vector $\mathbf{v}$ and $n \geq n_0$.

Proof:

First we note that if f is a density of an invariant measure μ of the map $x \to x^2 + a$ then $g(x, y) = f(x)f(y)$ is a density of an invariant measure of $T_{a,0}$, and the corresponding measure is the product measure. Moreover, by [28], for all $a_0 > -2$ there is a positive Lebesgue measure set E of values of the parameter a contained in $[-2, a_0]$ such that for any $a \in E$ the map $x \to L_a(x) = x^2 + a$ has an absolutely continuous and strongly mixing invariant measure μ, such that $\operatorname{supp}\mu = [a, a + a^2]$. This implies that for $a \in E$ the map $T_{a,0}$ has an absolutely continuous and ergodic invariant measure $\tilde{\mu} = \mu \times \mu$ (see e. g. [27]), with support equal to $R_a = [a, a + a^2] \times [a, a + a^2]$. In particular, $T_{a,0}|R_a$ is transitive (see e.g. [12], Prop. 2.8). Now, we will use the following result:

Lemma 4 *There exists a set $S \subset R_a$ such that $\tilde{\mu}(S) = 1$ and if $x \in S$ then its $T_{a,0}$-orbit is dense in R_a.*

Proof:

First, we observe that if $U \subset R_a$ is open and non-empty, then $\tilde{\mu}(\bigcup_{n\geq 0} T^{-n}_{a,0}(U)) > 0$. Let $\{U_n\}_{n\geq 0}$ be a countable basis of open sets. If we define $S_{i,n} = \bigcup_{j\geq i} T^{-j}_{a,0}(U_n)$, $S_n = \bigcap_{i\geq 0} S_{i,n}$ then

1. $S_{i,n} = T^{-1}_{a,0}(S_{i-1,n}) \subset S_{i-1,n}$, for all $i \geq 1$.

2. $\tilde{\mu}(S_n) = \lim_{i\to\infty} \tilde{\mu}(S_{i,n}) = \tilde{\mu}(S_{i,n}) > 0$, for all $i \geq 0$ and $n \geq 0$, because the measure is invariant.

3. S_n is a $T_{a,0}$-invariant set and, as $\tilde{\mu}$ is ergodic, $\tilde{\mu}(S_n) = 1$ for all $n \geq 0$.

4. S_n is residual, because as $T_{a,0}$ is transitive, then $S_{i,n}$ is open and dense, for all $n \geq 0$ and $i \geq 0$ (see Proposition 11.4 in [12]).

Now, if we define $S=\bigcap_{n\geq 0} S_n$, then, obviously, $\tilde{\mu}(S)=1$ is residual and, moreover, if $x\in S$ then its ω-limit $\omega(x)$ coincides with R_a. Indeed, it is enough to prove that, for all $n\geq 0$ there are infinitely many values $m>0$ for which $T_{a,0}^m(x)\in U_n$. But $x\in S$ implies that $x\in S_n$, that is

$$x\in\bigcap_{i\geq 0}\bigcup_{j\geq i} T_{a,0}^{-j}(U_n),$$

which means that $x\in T_{a,0}^{-m}(U_n)$ for infinitely many values m, and for these values $T_{a,0}^m(x)\in U_n$. This finishes the proof of the lemma. $\square$

In order to finish the proof of the proposition, let us define $W\subset[a,a+a^2]$ as the set of points $x\in[a,a+a^2]$ for which $\lambda(x)>0$, where

$$\lambda(x)=\limsup_{n\to\infty}\frac{1}{n}\log|DL_a^n(x)|.$$

As μ is absolutely continuous and ergodic then there exists $W_1\subset W$ such that $\mu(W_1)=1$ and $\lambda(x)=\Lambda=\int\log|DL_a|d\mu>0$, for all $x\in W_1$ (see e. g. Theorem 3.2, page 366 of [13]). Hence, if $\mathbf{v}\in\mathbb{R}^2$ is a nonzero vector and $(x,y)\in W_1\times W_1$ the Lyapounov exponent of $T_{a,0}$ at (x,y) in the direction of $\mathbf{v}$, which we denote by $\lambda_{\mathbf{v}}(x,y)$ is always equal to $\Lambda/2>0$. As $\tilde{\mu}(W_1\times W_1)=1$, we deduce that $(W_1\times W_1)\cap S\neq\emptyset$, meaning that there exists a dense orbit for which all the Lyapounov exponents are positive. In order to end the proof, we only have to take into account the behaviour of the Lyapounov exponent for the logistic map, when a is close to -2. $\square$

In order to find more values of the parameters a and b for which the existence of an invariant domain for the map $T_{a,b}$ can be proved, let us observe that there exist invariant lines for $T_{a,0}^2$. Hence, a possible way for finding attractors would be to detect those parameters (a,b) for which the respective map $T_{a,b}^2$ has invariant lines. Besides the case $b=0$, it can be shown that this fact happens when one takes a parameter in the curve G given by

$$G=\left\{(a\left(t\right),b\left(t\right))=\left(-\frac{1}{4}t^3\left(t^3-2t^2+2t-2\right),-t^2+t\right):t\in\mathbb{R}\right\}\tag{4}$$

being the respective invariant line for $T_{a,b}^2$ the one giving by

$$L^1=L^1\left(t\right)=\left\{(x,y)\in\mathbb{R}^2:x=A+By;A=\frac{1}{2}\left(t-t^2\right)t^2,\,B=t^2\right\}.$$

This invariant line contains the fixed point $P_{a,b}$ of $T_{a,b}$ (see (3)). Let us denote, for every t, by $C_1=C_1\left(t\right)$ the segment of L^1 joining $P_{a,b}$ with the point $L=(A,0)$. Then, one can show that, taking the parabola

$$L^2=L^2\left(t\right)=\left\{(x,y)\in\mathbb{R}^2:x=\left(\frac{y-A}{b+B}\right)^2+a\right\},$$

then L^2 contains $P_{a,b}$ and $T_{a,b}\left(C_1\right)\subset L^2$.

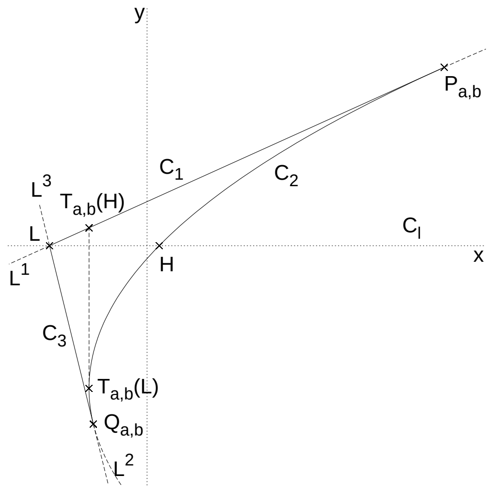

Figure 1: The shape of R_t, for $t < 2$.

On the other hand, if $Q_{a,b} = Q_{a,b}(t)$ is the unique point different from $P_{a,b}$ satisfying $T_{a,b}(Q_{a,b}) = P_{a,b}$, then $Q_{a,b}$ belongs to L^2 and, denoting by $C_2 = C_2(t)$ the segment on L^2 joining $Q_{a,b}$ with $P_{a,b}$ then $T_{a,b}(C_2) \subset L^1$.

Finally, denoting by

$$L^3 = L^3(t) = \left\{(x,y) \in \mathbb{R}^2 : x = A - (2b + B)\, y\right\}$$

it is easy to see that the points $L = (A, 0)$ and $Q_{a,b}$ belong to L^3 and, denoting by $C_3 = C_3(t)$ the segment on L^3 joining L with $Q_{a,b}$, then $T_{a,b}(C_3) \subset L^2$.

Let us denote, for every $(a(t), b(t)) \in G$, by R_t the bounded set limited by the segments C_1, C_2 and C_3, and by C_l the critical line, i.e., the straight line $y = 0$, for the transformation $T_{a,b}$. Then, it is easy to see that $T_{a,b}(R_t) \subset R_t$ whenever $T_{a,b}(C_l \cap R_t) \subset R_t$.

Let us observe that the set $C_l \cap R_t$ coincides with the line joining L with the point $H = H(t) = \left(\left(\frac{A}{b+B}\right)^2 + a, 0\right)$. Therefore, it is straightforward to see that condition $T_{a,b}(C_l \cap R_t) \subset R_t$ is fulfilled whenever $\left(\frac{A}{b+B}\right)^2 + a \geq 0$ (recall that the first image by $T_{a,b}$ of any segment in the critical line is a vertical straight segment and that the first image of the point H belongs to L^1 while the first image of the point L belongs to L^2).

The bigger value of t for which the condition $\left(\frac{A}{b+B}\right)^2 + a \geq 0$ holds corresponds to $t = 2$. In fact, for $t = 2$, or $(a, b) = (-4, -2)$, one has the limit case for which $T_{a,b}(R_t) \subset R_t$ (in fact, $T_{-4,-2}(R_2) = R_2$). After this limit situation there always exist critical points inside R_t whose orbits leave the domain R_t, which is no longer invariant. This is also the behaviour of the critical point of the quadratic one-dimensional family $Q_a(x) = 1 - ax^2$ for values of the parameter greater than 2.

2.2 The map $\mathbf{T}_{-4,-2}$

Let us begin by recalling that $Q_2(x) = 1 - 2x^2$ is a Misiurewicz map, i.e., the forward iterates of the critical point stay outside a fixed neigbourhood of the critical point. Furthermore, for this special Misiurewicz transformation it holds that all the positive images of the critical point belong to the boundary of the maximal invariant domain of Q_2, i.e., to the boundary of the interval $[-1,1]$. This is one of the reasons why the map Q_2 can be conjugate to the tent map $T : z \in [-1,1] \to T(z) = 1 - 2|z|$ via the change of coordinates $z = 4\pi^{-1} \arcsin\left(\sqrt{\frac{x+1}{2}}\right) - 1$. This fact gives a lot of information about the topological and ergodic behaviour of the orbits of Q_2, see for instance [4].

For our "limit" transformation $T_{-4,-2}$ we have that $P_{-4,-2} = (12,4)$, $L = (-4,0)$, $Q_{-4,-2} = (-4,-4)$, and $H = (0,0)$. Moreover, $T_{-4,-2}(C_l \cap R_2) = C_3$, $T_{-4,-2}(C_3) = C_2$, $T_{-4,-2}(C_2) = C_1$ and $T_{-4,-2}(C_1) = C_2$. Therefore, all the positive iterates of any critical point belong to the boundary of the maximal invariant domain R_2. This would be enough in order to check that $T_{-4,-2}$ is conjugate to some bidimensional map displaying all the nice properties exhibited by the unidimensional tent map (for instance, constant jacobian outside critical points).

In fact, it is easy to see that the restriction of $T^2_{-4,-2}$ to its invariant segment C_1 is conjugate to the transformation

$$\theta \in [0,4] \to \lambda(\theta) = (2-\theta)^2,$$

which is also a Misiurewicz unimodal map conjugate to a unidimensional standard tent map.

In order to extend these ideas to the whole domain of definition of $T_{-4,-2}$ let us define on R_2 the change of coordinates

$$(x,y) \to (X,Y) = \left(\frac{1}{2}\left(y - \sqrt{y^2+8y-4x}\right), \frac{1}{2}\left(y + \sqrt{y^2+8y-4x}\right)\right). \tag{5}$$

Under this change of variables it is easy to see that the $T_{-4,-2}$-invariant region R_2 becomes into the triangle

$$\mathcal{A} = \{(X,Y) : -2 \leq X \leq 2,\ X \leq Y \leq 2\}$$

where the respective transformation, denoted by $\widetilde{T}$, is defined by

$$\widetilde{T}(X,Y) = \begin{pmatrix} \frac{1}{2}\left(XY - \sqrt{(4-X^2)(4-Y^2)}\right) \\ \frac{1}{2}\left(XY + \sqrt{(4-X^2)(4-Y^2)}\right) \end{pmatrix}$$

The new change of coordinates defined in $\mathcal{A}$

$$(X,Y) \to (\Phi,\Psi) = \left(\arccos\left(\frac{X}{2}\right), \arccos\left(\frac{Y}{2}\right)\right), \tag{6}$$

where $\arccos : z \in [-1,1] \to \arccos(z) \in [0,\pi]$, transforms $\mathcal{A}$ into

$$\mathcal{B} = \{(\Phi,\Psi) : 0 \leq \Phi \leq \pi,\ 0 \leq \Psi \leq \Phi\}$$

while, in this new coordinates, $T_{-4,-2}$ is written as

$$\Lambda(\Phi,\Psi) = (\pi - |\pi - \Phi - \Psi|, \Phi - \Psi).$$

Remark 5 *Let us denote by Γ the composition of the transformations given in (5) and (6). Then, it is easy to see that Γ^{-1} is defined by*

$$(x,y) = \Gamma^{-1}(\Phi,\Psi) = (4(\cos\Phi + \cos\Psi + \cos\Phi\cos\Psi), 2(\cos\Phi + \cos\Psi)).$$

Therefore, Γ^{-1} is a C^1-map defined on $\mathcal{B}$.

Let us observe that the critical line for $T_{-4,-2}$ is mapped by Γ into the line $\Phi + \Psi = \pi$ (the set in which Λ is not smooth). Let us denote by $\mathcal{C}$ the points in $\mathcal{B}$ belonging to this critical line. We point out that outside this critical set $\mathcal{C}$ the entries of the matrix $D\Lambda$ are constants. We also remark that the boundary of $\mathcal{B}$ is Λ-invariant and contains the set $\bigcup_{n>0}\Lambda^n(\mathcal{C})$. Therefore, the map Λ would display the same properties as the unidimensional tent map.

2.3 The bidimensional tent map Λ

The aim of this paragraph is to check that, in fact, the map Λ is conjugate to a shift defined on a subset of the space of sequences of two symbols:

$$\mathcal{S} = \{\mathcal{X} : n \in \mathbb{N} \to \mathcal{X}(n) \in \{0,1\}\}. \tag{7}$$

Let us begin by observing that the critical set $\mathcal{C}$ of Λ divides $\mathcal{B}$ into two disjoint triangles A_0 and A_1 defined by

$$A_0 = \{(\Phi,\Psi) \in \mathcal{B} : \Phi + \Psi \le \pi\},\ A_1 = \mathcal{B}\backslash A_0 \tag{8}$$

and, furthermore, it follows that $\Lambda(A_0) = \mathcal{B}$ and $\Lambda(A_1) = \mathcal{B}\backslash\Lambda(\mathcal{C})$.

Now, let us consider the first two preimages of $\mathcal{C}$. These preimages are the straight segments in $\mathcal{B}$ given by the equations $\Phi = \frac{\pi}{2}$ and $\Psi = \frac{\pi}{2}$. Therefore, these preimages of $\mathcal{C}$ divide each one of the sets A_0 and A_1 into two new triangles. These four triangles are denoted by A_{00}, A_{01}, A_{10} and A_{11} according to the following rule: $A_{ij} \subset A_i$ and $\Lambda(A_{ij}) = A_j$ for $i,j = 0,1$. In this way, we get, for each $n \in \mathbb{N}$, a partition $\{A_{x_1x_2...x_n} : x_k \in \{0,1\}, k = 1,...,n\}$ of $\mathcal{B}$ by 2^n triangles recurrently defined by the following two conditions:

1.- $A_{x_1x_2...x_n} \subset A_{x_1x_2...x_{n-1}}$.

2.- $\Lambda^{n-1}(A_{x_1x_2...x_n}) = \Lambda^{n-2}(A_{x_2x_3...x_n}) = ... = \Lambda\left(A_{x_{n-1}x_n}\right) = A_{x_n}$.

In Figure 2 we have drawn the partition of $\mathcal{B}$ for $n = 3$.

Let us define

$$P_{\{x_n\}} = A_{x_1x_2...} = \bigcap_{j\in\mathbb{N}} A_{x_1x_2...x_j}$$

for each $\{x_n\}_{n\in\mathbb{N}} \in \mathcal{S}$, see (7).

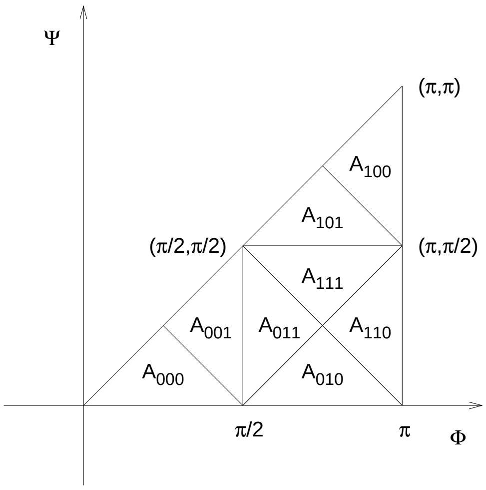

Figure 2: The partition of $\mathcal{B}$ for $n = 3$.

Since the triangles $A_{x_1 x_2 \ldots x_j}$ are convex sets and $diam.\left(A_{x_1 x_2 \ldots x_j}\right) \to 0$ as $j \to \infty$, it follows that, for each sequence $\{x_n\}_{n\in\mathbb{N}} \in \mathcal{S}$, $P_{\{x_n\}}$ is a point in $\mathcal{B}$.

One can see that there exist different sequences in $\mathcal{S}$ giving rise to the same point in $\mathcal{B}$. For instance, if one takes $\{x_n\} = \{1, 1, 0, 0, 0, \ldots\}$ and $\{y_n\} = \{0, 1, 0, 0, 0, \ldots\}$ then $P_{\{x_n\}} = P_{\{y_n\}} = (\pi, 0)$. Since our purpose is to construct a conjugation between Λ and a shift defined on same part of $\mathcal{S}$, we must avoid certain class of sequences by bearing in mind that only the critical line $\mathcal{C}$ is mapped by Λ into the straight line $\{(\Phi, \Psi) \in \mathcal{B} : \Phi = \pi\}$. Therefore, recalling that, by construction, see (8), the critical set $\mathcal{C}$ is contained in A_0, we introduce the subset $\mathcal{S}^*$ of $\mathcal{S}$ defined by the following three conditions:

1.- If $x_2 = 1$ and $x_j = 0$ for every $j > 2$, then $\{x_n\}_{n\in\mathbb{N}} \in \mathcal{S}^*$ if and only if $x_1 = 0$. We are describing by this condition the orbit of the point $(\pi, 0)$.

2.- If there exists $n_0 > 2$ for which $x_{n_0} = 1$ and $x_j = 0$ for every $j > n_0$, then $\{x_n\}_{n\in\mathbb{N}} \in \mathcal{S}^*$ if and only if $x_{n_0-1} = x_{n_0-2} = 0$. We are describing the orbit of the preimages of $(\pi, 0)$.

3.- If there exists $n_0 > 1$ for which $x_{n_0} = 1$ and $x_{n_0+2j} = 0$ for every $j > 1$, then $\{x_n\}_{n\in\mathbb{N}} \in \mathcal{S}^*$ if and only if $x_{n_0-1} = 0$. We are describing the orbit of every preimage of each critical point different from $\left(\frac{\pi}{2}, \frac{\pi}{2}\right)$ and $(\pi, 0)$.

Then, one can show that the map

$$h : \{x_n\} \in \mathcal{S}^* \to h\left(\{x_n\}\right) = P_{\{x_n\}} \in \mathcal{B} \tag{9}$$

is one to one and onto. Moreover, classical arguments allow us to show that h is continuous when considering the metric in $\mathcal{S}^*$ induced by the distance

$$d\left(\{x_n\}, \{y_n\}\right) = \sum_{i\in\mathbb{N}} \frac{1}{2^i} \left|x_i - y_i\right|. \tag{10}$$

Finally, considering on $\mathcal{S}^*$ the shift transformation Θ defined, as usually, by $\Theta(\{x_n\}) = \{y_n\}$ with $y_n = x_{n+1}$, it is easy to see that $\Lambda \circ h = h \circ \Theta$ (observe that $\Theta(\mathcal{S}^*) \subset \mathcal{S}^*$). This is the main reason why we call the map Λ the **bidimensional tent map**.

2.4 Properties of the map $T_{-4,-2}$

Now, as in the unidimensional setting, from the fact that $T_{-4,-2}$ is conjugate (via the composition of (5), (6) and (9)) to the shift transformation Θ we may derive several properties for the maps Λ and $T_{-4,-2}$:

1.- Since for every $p \in \mathbb{N}$ the map Θ has periodic orbits of period p and the set of periodic orbits of Θ is dense in $\mathcal{S}^*$, the same holds for the maps Λ on $\mathcal{B}$ and $T_{-4,-2}$ on R_2.

2.- The two fixed points of $T_{-4,-2}$, $P_{-4,-2} = (12, 4)$ and $\widetilde{P}_{-4,-2} = (-3, -1)$ satisfy $\overline{W^u(P_{-4,-2})} = \overline{W^u\left(\widetilde{P}_{-4,-2}\right)} = R_2$ and the two fixed points of Λ, $(0, 0)$ and $\left(\frac{4}{5}\pi, \frac{2}{5}\pi\right)$ satisfy $\overline{W^u((0,0))} = \overline{W^u\left(\left(\frac{4}{5}\pi, \frac{2}{5}\pi\right)\right)} = \mathcal{B}$. This follows from the fact that the same holds for the two fixed points of Θ. In fact, in order to prove that the unstable set of the fixed point $\{1, 1, 1, ...\}$ of Θ is dense in $\mathcal{S}^*$, let us choose any sequence $\{x_n\} \in \mathcal{S}^*$ and define, for every $j \in \mathbb{N}$, the element of $\mathcal{S}^*$ given by

$$\{y_n^j\} = \begin{cases} 1, \text{ if } n \leq j \\ x_{n-j}, \text{ if } n > j \end{cases}$$

Then, it is easy to check, see (10), that $d(\{1, 1, 1, ...\}, \{y_n^j\}) \to 0$ as $j \to \infty$ and, moreover, that $\Theta^j(\{y_n^j\}) = \{x_n\}$. Of course, in the same way, one may prove that the unstable set of any point in $\mathcal{S}^*$ is dense in $\mathcal{S}^*$. Hence, the unstable manifold (with respect to the transformation Λ) of any point in $\mathcal{B}$ is dense in $\mathcal{B}$ and the unstable manifold (with respect to the transformation $T_{-4,-2}$) of any point in R_2 is dense in R_2.

3.- The map Λ has dense orbits in $\mathcal{B}$ and the map $T_{-4,-2}$ has dense orbits in R_2. These are direct consequences of the fact that the same holds for the map Θ in $\mathcal{S}^*$. Of course, recalling that we have denoted by $\mathcal{C}$ the critical set of the map Λ, from the fact that $\Lambda^n(\mathcal{C})$ is contained in the boundary of $\mathcal{B}$ for every $n \in \mathbb{N}$, it follows that no dense orbit of Λ intersects the critical line $\mathcal{C}$. On the other hand, we have that

$$D\Lambda(\Phi, \Psi) = \begin{pmatrix} 1 & 1 \\ 1 & -1 \end{pmatrix} \text{ and } D\Lambda(\Phi, \Psi) = \begin{pmatrix} -1 & -1 \\ 1 & -1 \end{pmatrix} \tag{11}$$

in the respective cases in which $(\Phi, \Psi) \in A_0 \backslash \mathcal{C}$ or $(\Phi, \Psi) \in A_1$ (see (8)). Therefore, if the Λ-orbit of (Φ_0, Ψ_0) is dense in $\mathcal{B}$ the two Lyapounov exponents of Λ along $\{\Lambda^n(\Phi_0, \Psi_0) : n \in \mathbb{N}\}$ are positive. More concretely, it is straightforward to check that, for every unit vector $\mathbf{v}$, one has

$$\|D\Lambda^n(\Phi_0, \Psi_0)\mathbf{v}\| = \left(\sqrt{2}\right)^n.$$

Therefore, according to Definition 2 the whole $\mathcal{B}$ is a strange attractor for the transformation Λ.

4.- For any $n \in \mathbb{N}$, nor Λ^n neither $T^n_{-4,-2}$ are C^1-conjugate to any map of the type $H(x,y) = (H_1(x), H_2(x,y))$. This is a direct consequence of the fact that $T_{-4,-2}$ and Λ have periodic orbits of any period and with complex eigenvalues. To check this claim it is enough to prove it for the map Λ (we have already pointed out, see Remark 5, that the inverse of the composition of the maps given in (5) and (6) is smooth).

Hence, let p be any natural number. In order to prove that Λ has a periodic point of period p with complex eigenvalues, let us observe that, according to (11), if (Φ_0, Ψ_0) is a point in A_0 such that $(\Phi_1, \Psi_1) = \Lambda(\Phi_0, \Psi_0) \in A_0$, then $D\Lambda^2(\Phi_0, \Psi_0) = 2I_d$, where I_d is the identity matrix. On the other hand, if (Φ_0, Ψ_0) is a point in A_1 such that $(\Phi_1, \Psi_1) = \Lambda(\Phi_0, \Psi_0) \in A_1$, then, see (11), the eigenvalues of $D\Lambda(\Phi_0, \Psi_0)$ are $-1 \pm i$, while the eigenvalues of $D\Lambda^2(\Phi_0, \Psi_0)$ are $\pm 2i$.

Therefore, if p is odd it is enough to take a periodic orbit of period p spending $p-1$ iterates in A_0 and just one iterate in A_1 (recall that this choice is always possible due to the fact that Λ is conjugate to the shift map Θ). On the other hand, if p is even it suffices to choose a periodic orbit of period p spending $p-2$ iterates in A_0 and two iterates in A_1.

Before stating our last property for the maps $T_{-4,-2}$ and Λ, let us summarize the main conclusion derived from the last two properties described above:

Remark 6 *As far as we know, the map Λ is the first example of bidimensional transformation satisfying the following two properties:*

a) For each $n \in \mathbb{N}$, Λ^n is not C^1-conjugate to any map of the type

$$H(x,y) = (H_1(x), H_2(x,y)).$$

b) The map Λ exhibits a two-dimensional strange attractor with two positive Lyapounov exponents.

We finish this paragraph by stating certain ergodic properties for the maps $T_{-4,-2}$ and Λ:

Proposition 7 *Let $D : \mathbb{T}^2 \to \mathbb{T}^2$ be such that $D(x,y) = (2x, 2y) \mod 2\pi$, for $(x,y) \in \mathbb{T}^2 = \{(x,y) \mod 2\pi\}$. Then D is topologically semi-conjugate to $\Lambda^2|\mathcal{B}$.*

Proof:

First we define a surjective map $\rho : \mathbb{T}^2 \to \mathcal{B}$: Let $(x,y) \in \mathbb{R}^2$ be a representative of a point in $\mathbb{T}^2$ such that $-\pi \leq x \leq \pi$ and $-\pi \leq y \leq \pi$. Then we define

$$\rho(x,y) = \begin{cases} (|x|, |y|) & \text{if} \quad |x| \geq |y| \\ (|y|, |x|) & \text{if} \quad |x| \leq |y| \end{cases}$$

In order to prove that $\rho\circ D=\Lambda^2\circ\rho$, we recover some elements of the partion of $\mathcal{B}$ defined in Section 2.3:

$$\begin{aligned}
A_{00} &= \{(\Phi,\Psi)\mid 0\le\Phi\le\pi/2,\ 0\le\Psi\le\Phi\}\\
A_{01} &= \{(\Phi,\Psi)\mid \pi/2\le\Phi\le\pi,\ 0\le\Psi\le\pi-\Phi\}\\
A_{11} &= \{(\Phi,\Psi)\mid \pi/2\le\Phi\le\pi,\ \pi-\Phi\le\Psi\le\pi/2\}\\
A_{10} &= \{(\Phi,\Psi)\mid \pi/2\le\Phi\le\pi,\ \pi/2\le\Psi\le\Phi\}
\end{aligned}$$

This sets are drawn in Figure 3. We recall that if

$$\begin{aligned}
A_0 &= \{(\Phi,\Psi)\mid 0\le\Psi\le\pi/2,\ \Psi\le\Phi\le\pi-\Psi\},\\
A_1 &= \{(\Phi,\Psi)\mid \pi/2\le\Phi\le\pi,\ \pi-\Phi\le\Psi\le\Phi\},
\end{aligned}$$

then $\Lambda(A_{00})=A_0$, $\Lambda(A_{01})=A_1$, $\Lambda(A_{11})=A_1$ and $\Lambda(A_{10})=A_0$. Therefore:

$$\Lambda^2(\Phi,\Psi)=\begin{cases}(2\Phi,2\Psi) & \text{if } (\Phi,\Psi)\in A_{00}\\ (2\pi-2\Phi,2\Psi) & \text{if } (\Phi,\Psi)\in A_{01}\\ (2\Psi,2\pi-2\Phi) & \text{if } (\Phi,\Psi)\in A_{11}\\ (2\pi-2\Psi,2\pi-2\Phi) & \text{if } (\Phi,\Psi)\in A_{10}\end{cases}$$

Let (x,y) be a representative of a point in $\mathbb{T}^2$, such that $-\pi\le x\le\pi$, $-\pi\le y\le\pi$. We want to prove that

$$\rho(D(x,y))=\Lambda^2(\rho(x,y)). \tag{12}$$

In all the computations below, we shall always take the representative of a point in $\mathbb{T}^2$, in the rectangle $[-\pi,\pi]\times[-\pi,\pi]$. We distinguish between several cases:

1. $(|x|,|y|)\in A_{00}$: This means that $D(x,y)=(2x,2y)$, $\rho(D(x,y))=(2|x|,2|y|)$, since $(2|x|,2|y|)\in\mathcal{B}$, and $\Lambda^2(\rho(x,y))=\Lambda^2(|x|,|y|)=(2|x|,2|y|)$. Hence, (12) holds.

2. $(|y|,|x|)\in A_{00}$: In this case $\rho(D(x,y))=\rho(2x,2y)=(2|y|,2|x|)$ and $\Lambda^2(\rho(x,y))=\Lambda^2(|y|,|x|)=(2|y|,2|x|)$.

3. $(x,|y|)\in A_{01}$: Here $\rho(D(x,y))=\rho(2x-2\pi,2y)=(2\pi-2x,2|y|)$ and $\Lambda^2(\rho(x,y))=\Lambda^2(x,|y|)=(2\pi-2x,2|y|)$.

4. $(-x,|y|)\in A_{01}$: We have $\rho(D(x,y))=\rho(2x+2\pi,2y)=(2\pi+2x,2|y|)$ and $\Lambda^2(\rho(x,y))=\Lambda^2(-x,|y|)=(2\pi+2x,2|y|)$.

5. $(y,|x|)\in A_{01}$: This implies that $\rho(D(x,y))=\rho(2x,2y-2\pi)=(2\pi-2y,2|x|)$ and $\Lambda^2(\rho(x,y))=\Lambda^2(y,|x|)=(2\pi-2y,2|x|)$.

6. $(-y,|x|)\in A_{01}$: Then $\Lambda^2(\rho(x,y))=\rho(D(x,y))=(2\pi+2y,2|x|)$.

7. $(x,|y|)\in A_{11}$: In this case, $\rho(D(x,y))=\rho(2x-2\pi,2y)=(2|y|,2\pi-2x)$ and $\Lambda^2(\rho(x,y))=\Lambda^2(x,|y|)=(2|y|,2\pi-2x)$.

8. $(-x,|y|)\in A_{11}$: We have $\rho(D(x,y))=\rho(2\pi+2x,2y)=(2|y|,2\pi+2x)$ and $\Lambda^2(\rho(x,y))=\Lambda^2(-x,|y|)=(2|y|,2\pi+2x)$.

9. $(y,|x|) \in A_{11}$: Here, $\rho(D(x,y)) = \rho(2x, 2y-2\pi) = (2|x|, 2\pi-2y)$ and $\Lambda^2(\rho(x,y)) = \Lambda^2(y,|x|) = (2|x|, 2\pi-2y)$.

10. $(-y,|x|) \in A_{11}$: In this case, $\rho(D(x,y)) = \rho(2x, 2y+2\pi) = (2|x|, 2y+2\pi)$ and $\Lambda^2(\rho(x,y)) = \Lambda^2(-y,|x|) = (2|x|, 2\pi+2y)$.

11. $(x,y) \in A_{10}$: Then, $\rho(D(x,y)) = \rho(2x-2\pi, 2y-2\pi) = (2\pi-2y, 2\pi-2x)$ and $\Lambda^2(\rho(x,y)) = \Lambda^2(x,y) = (2\pi-2y, 2\pi-2x)$.

12. $(-x,y) \in A_{10}$: Here, $\rho(D(x,y)) = \rho(2x+2\pi, 2y-2\pi) = (2\pi-2y, 2\pi+2x)$ and $\Lambda^2(\rho(x,y)) = \Lambda^2(-x,y) = (2\pi-2y, 2\pi+2x)$.

13. $(x,-y) \in A_{10}$: We have, $\rho(D(x,y)) = \rho(2x-2\pi, 2y+2\pi) = (2\pi+2y, 2\pi-2x)$ and $\Lambda^2(\rho(x,y)) = \Lambda^2(x,-y) = (2\pi+2y, 2\pi-2x)$.

14. $(-x,-y) \in A_{10}$: In this case, $\rho(D(x,y)) = \rho(2x+2\pi, 2y+2\pi) = (2y+2\pi, 2x+2\pi)$ and $\Lambda^2(\rho(x,y)) = \Lambda^2(-x,-y) = (2\pi+2y, 2\pi+2y)$.

15. $(y,x) \in A_{10}$: Here, $\rho(D(x,y)) = \rho(2x-2\pi, 2y-2\pi) = (2\pi-2x, 2\pi-2y)$ and $\Lambda^2(\rho(x,y)) = \Lambda^2(y,x) = (2\pi-2x, 2\pi-2y)$.

16. $(y,-x) \in A_{10}$: This implies that $\rho(D(x,y)) = \rho(2\pi+2x, 2y-2\pi) = (2\pi+2x, 2\pi-2y)$ and $\Lambda^2(\rho(x,y)) = \Lambda^2(y,-x) = (2\pi+2x, 2\pi-2y)$.

17. $(-y,x) \in A_{10}$: We have, $\rho(D(x,y)) = \rho(2x-2\pi, 2y+2\pi) = (2\pi-2x, 2\pi+2y)$ and $\Lambda^2(\rho(x,y)) = \Lambda^2(-y,x) = (2\pi-2x, 2\pi+2y)$.

18. $(-y,-x) \in A_{10}$: Here, $\rho(D(x,y)) = \rho(2\pi+2x, 2\pi+2y) = (2\pi+2x, 2\pi+2y)$ and $\Lambda^2(\rho(x,y)) = \Lambda^2(-y,-x) = (2\pi+2x, 2\pi+2y)$.

All these cases implies that (12) is true for all $(x,y) \in \mathbb{T}^2$. $\square$

Corollary 8 *The Lebesgue measure is ergodic with respect to the map Λ, and $T_{-4,-2}$ has an invariant absolutely continuous and ergodic measure defined by the density:*

$$\bar{\rho}\,(x,y) = \frac{1}{\pi^2\sqrt{4+x-4y}\sqrt{\frac{1}{4}y^2+2y-x}\sqrt{x+4}}.$$

Proof:

The ergodicity of the Lebesgue measure with respect to Λ is a direct consequence of the ergodicity of the Lebesgue measure with respect to D and the previous proposition. The ergodicity of the measure with density $\bar{\rho}$, that we call μ, is due to the fact that, for all borelian subset $E \subset R_2$, it follows that $\mu(E) = \lambda(\Gamma^{-1}(E))$, where λ is the normalized Lebesgue measure in $\mathcal{B}$ and Γ^{-1} is the map defined in Remark 5. $\square$

Finally, the fact that $T_{-4,-2}$ is conjugate to Λ and, therefore, the set of dense orbits has total measure in R_2, implies the following proposition:

Proposition 9 *For almost all $x \in R_2$ and all $\mathbf{v} \in \mathbb{R}^2$ different form zero, the Lyapounov exponent of x with respect to $T_{-4,-2}$, in the direction of $\mathbf{v}$, is $\frac{1}{2}\log 2$.*

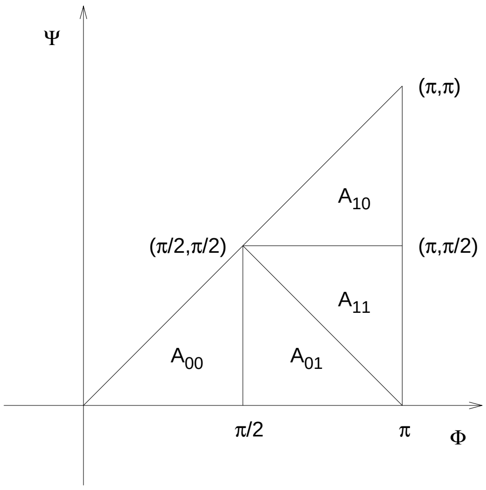

Figure 3: The partition of $\mathcal{B}$ in the sets A_{ij}, $0 \leq i \leq 1$ and $0 \leq j \leq 1$.

2.5 Open questions

It seems clear that the map $T_{-4,-2}$ displays the same properties that of the unidimensional Misiurewicz map $Q_2(x) = 1 - 2x^2$. Therefore, guided by the results proving the existence of strange attractors for a subset of positive Lebesgue measure on the space of parameters in the case of the logistic family, see [1], [2] and [9], or by the respective extensions to more generic families of unidimensional maps, see [13], we state Conjecture 10.

This conjecture establishes the existence, with positive probability in the curve of parameters G given in (4), of two-dimensional strange attractors with two positive Lyapounov exponents for the respective transformation $T_{a(t),b(t)}$ defined in R_t. As in the unidimensional case, this set of parameters would be located close enough to the Misiurewicz value $t = 2$:

Conjecture 10 *For any* $0 < c < \frac{1}{2}\log 2$ *there exists* $t_0 < 2$ *and a positive Lebesgue measure set* E *of values of the parameter* t *contained in* $[t_0, 2]$ *such that for any* $t \in E$ *there exists a dense orbit* $\bigcup_{n\in\mathbb{N}} \left\{T^n_{a,b}(x_0, y_0)\right\}$ *in* R_t*,* $(a,b) = (a(t), b(t)) \in G$*, such that*

$$\left\| DT^n_{a,b}(x_0, y_0)\,\mathbf{v}\right\| \geq e^{cn},$$

for any unit vector $\mathbf{v}$*.*

We finish this section with a new conjecture, see Conjecture 11. This conjecture claims that the existence of two-dimensional strange attractors would be a phenomenon of positive probability in the space of parameters when a two parameter family of three-dimensional diffeomorphisms unfolds a homoclinic tangency in case B (in (1) the associated limit return maps are written). This would be a natural extension of the results given in [15] for two-dimensional diffeomorphisms. Let us recall that we refer the reader to [24] to obtain the statement of the linearization assumption and the definition of generalized homoclinic tangency.

Conjecture 11 *Let $\{f_{a,b}\}_{a,b}$ be a two parameter family of three-dimensional diffeomorphisms and suppose that f_{a_0,b_0} has a dissipative saddle fixed point p_0. Assume that the family $\{f_{a,b}\}_{a,b}$ satisfies the linearization assumption and that the eigenvalues λ_1, λ_2 and λ_3 of $Df_{a_0,b_0}(p_0)$ satisfy $|\lambda_1| < 1$ and $|\lambda_3| > |\lambda_2| > 1$. If the invariant manifolds of p_0 have a generalized homoclinic tangency for $(a,b) = (a_0,b_0)$ which unfolds generically, then there exists a positive measure set E of parameter values near (a_0,b_0), such that for $(a,b) \in E$ the diffeomorphism $f_{a,b}$ exhibits a strange attractor with two positive Lyapounov exponents.*

Of course, a proof for Conjecture 10 would be a first step in order to prove Conjecture 11. At least, this was the route to prove the persistence of strange attractors for two-dimensional transformations in [2], [15], [19], [20], among others: Take advantage of the respective unidimensional results given for example in [1],[9], [19] (Chapter 2).

3 Numerical examples

In this section we introduce some numerical experiments showing the geometry of certain attractors arising in the invariant domain R_t of $T_{a,b}$, $(a,b) \in G$ (see(4)), for different values of $t \in (1.8, 2)$ (recall that, if $t = 2$ then $(a,b) = (-4,-2)$). Previously, we define the following change of coordinates depending on the parameter t transforming, for every $t \in G$, the invariant region R_t into R_2:

$$(x,y,t) \to \left(\overline{x},\overline{y},\overline{t}\right) = \left(\frac{16}{t^4}x + \frac{16\,(2-t)}{t^3}y + 4 - \frac{8}{t}, \frac{8}{t^3}y, t\right).$$

In this new coordinates the map $T_{a,b}$ is denoted by $\overline{T}_{a,b}$ and is given by

$$\overline{T}_{a,b}\left(\overline{x},\overline{y}\right) = \left(\begin{array}{c} \frac{1}{4}t^2\overline{y}^2 + (2-t)\,t\overline{x} + 2\,(t-2)\,t\overline{y} + 12 - 8t \\ \frac{1}{2}t\overline{x} - t\overline{y} + 2\,(2-t) \end{array}\right). \tag{13}$$

We remark that the new parameter $\overline{t}$ coincides with the old one t. Hence, no new considerations are needed for the "old" curve of parameters G. In the future, we still denote by t the considered parameter on G and by T_t the respective transformation defined in (13), for which the maximal invariant set is R_2, independently of the value of t. We also remark that all the numerical experiments showed in this section were designed by taking ten initial conditions uniformly distributed on the critical set of T_t. It is straightforward to check that this critical set still corresponds to those points in R_2 for which $\overline{y} = 0$.

In each one of the forthcoming pictures and after dropping an initial transient (generally 10^6 initial iterates) we show bewteen 10000 and 40000 consecutive iterates of each one of the ten orbits mentioned above. We are also able to numerically detect periodic orbits and compute the respective eigenvalues. Furthermore, the Lyapounov exponents for each one of the obtained attractors can also be numerically approximated with an error of the order of 10^{-4}.

We start our analysis by pointed out that, for every $t \in (1.8, 1.8105)$, the attractor for T_t in R_2 reduces to a fixed point which corresponds to the fixed point $\widetilde{P}_{a,b}$ given in (3). This is completely equivalent to what happens for the quadratic unidimensional family $Q_a(x) = 1 - ax^2$ for values of the parameter a smaller than 0.75. Nevertheless, for $t \in (1.8, 1.8105)$, our attracting fixed point is a focus and for some value of the parameter t^* in $(1.8105, 1.8106)$ a Hopf bifurcation occurs. Therefore, an invariant circle springs and we denote it by IC (we follow here the terminology used in [6]). This set IC becomes an attractor for every $t \in (t^*, 1.8649)$ which cuts the critical line $y = 0$ for some value close to $t = 1.84275$ (henceforth, for this value of the parameter the attractor of T_t contains critical points, just in the same way as the quadratic unidimensional family does for $a = 1$ and also for slightly larger values than 1). The set IC for $t = 1.8428$ is the attractor represented in Figure 4 a).

This kind of attractors (invariant circles) were also observed in [6] when the two parameter family of bidimensional noninvertible maps

$$L_{a,\tau}(x, y) = \left((1 + a\tau)\, x - \tau xy, (1 - \tau)\, y + \tau x^2\right) \tag{14}$$

is numerically studied for values of the parameters a, τ belonging to certain line. This bidimensional family originally appears in a paper of Lorenz, see [11], in which the author studied a sequence of transitions from an attracting fixed point to "computational chaos" (chaotic attractors). These transitions evolved from an attracting fixed point to an attracting invariant circle (IC), and finally to a chaotic attractor. In view of the results obtained in [11], or even similar ones previously obtained in other noninvertible bidimensional cases, see [14], [22] or even [6], it was suggested that this would be a universal "noninvertible route to chaos". Therefore, the way in which these invariant circles disappear becomes a natural question in this scenario.

We refer the reader to [6] in which the mechanisms of creation and destruction of invariant circles are described in the invertible and noninvertible frameworks. For the invertible case we also cite [3], in which a complete description of those mechanisms is included. As for the noninvertible case, we remark that, in [11], the following scenario for a transition of a smooth IC to a chaotic attractor is proposed as the simplest possible one: As the parameter increases, the IC successively farther over the critical curve, causing it to develop successively sharper features. Nevertheless, we do not detect these sharper features for our attracting IC for values of the parameter t in $(t^*, 1.8649)$. Our IC is no longer a minimal attractor when the parameter t crosses certain value $t_0 \in (1.8649, 1.86492)$. For this parameter t_0 an attracting periodic node of period eight appears due to a saddle-node bifurcation. This attracting periodic orbit survives in the range of parameters $(t_0, 1.88165)$, but for some value in the above interval their eigenvalues become complex. In any case, beyond $t = t_0$, we do not "see" the set IC showed in Figure 4 a) anymore. Moreover, the IC becomes only continuous (see [3]) until the attracting periodic orbit undergoes a Hopf bifurcation, when a 8-pieces attracting invariant curve appears.

However, the presence of invariant circles developing sharper features, as was described in [11] and [6], becomes patent also in our situation for greater values of the parameter: In

Figure 4 e) it is shown the shape of one piece of an 8-pieces strange attractor that emerges from the eight periodic orbit arising at $t = t_0$. Namely, the periodic orbit described above undergoes a new Hopf bifurcation for some value of the parameter t in $(1.88165, 1.88166)$ giving rise to an attractor formed by eight invariant circles, that we denote by IC8. Figure 4 b) shows IC8 for $t = 1.88624$ (see also Figure 4 c), in which an amplification of one of these eight pieces is shown).

In order to follow the transition from Figure 4 c) ($t = 1.88624$) to Figure 4 e) ($t = 1.88762$) we refer the reader once again to [6] were the authors definitively associate the destruction of IC´s for the family given in (14) to the presence of global bifurcations, i.e., homoclinic or heteroclinic bifurcations (created from the intersections of invariant manifolds of periodic orbits which stay very close to the IC) which precede to the reappearance of an attractor, this time chaotic with loops (see Figure 4 e), where the piece of the attractor is no more homeomorphic to a circle). In fact, see [5], loops and cusps are usually observed on invariant curves for noninvertible maps. Of course, the existence of homoclinic bifurcations leads to the presence of high–periodic attractors and probably (one-dimensional) strange attractors, see [15]. This would explain the shape of the attractor represented in Figure 4 d) for the value of the parameter $t = 1.88758$. For this special value of the parameter we numerically obtain one probably positive Lyapounov exponent: In fact this numerical value corresponds to 2.13×10^{-4} (recall that we numerically approximate Lyapounov exponents with an error less than 10^{-4}).

Once the IC8 disappears the attractor becomes chaotic, see Figure 4 f) in which the continuation of the piece of the 8-pieces previous attractor is shown. The sum of the Lyapounov exponents for this value of the parameter ($t = 1.88773$) is positive. In fact, the numerically obtained exponents are 1.51×10^{-3} and -9.077×10^{-4}.

Therefore, at sight of the six pictures appearing in Figure 4 it seems clear that the transition from periodic attractors to chaotic attractors is a phenomenon which must occur not only for the bidimensional families studied in [6] and [11], but also in simpler situations (observe that our family (2) is substantially less complicated than the one given in (14)) and, even more important, in more generic situations: Three-dimensional diffeomorphisms unfolding homoclinic tangencies associated to fixed points whose unstable manifold has dimension two.

Furthermore, by increasing the value of t we also obtain more interesting situations which we are going to describe. In Figure 5, one may observe how two different attractors coexist for $t = 1.889$. One of them (the one displaying a bidimensional structure) is the continuation of the attractor described in Figure 4 f) and therefore is one of the pieces of an 8-pieces bidimensional attractor. A numerical analysis gives two positive Lyapounov exponents for this 2D attractor. From the topological point of view it is interesting to note that, for $t = 1.889$, the inner hole exhibited by the attractor in Figure 4 f) disappears (this phenomenon is frequently observed for our family T_t in several subdomains of the range of parameters $(1.8, 2)$). This also happens in the quadratic family for values of the parameter slightly bigger than 1, for which the attractor lives in two disjoint intervals leaving the fixed point (which is a repellor) between them. Moreover, the boundary of those intervals are positive iterates of the critical point. As increasing the parameter for the quadratic unidimensional family $Q_a(x) = 1 - ax^2$ these disjoint intervals containing

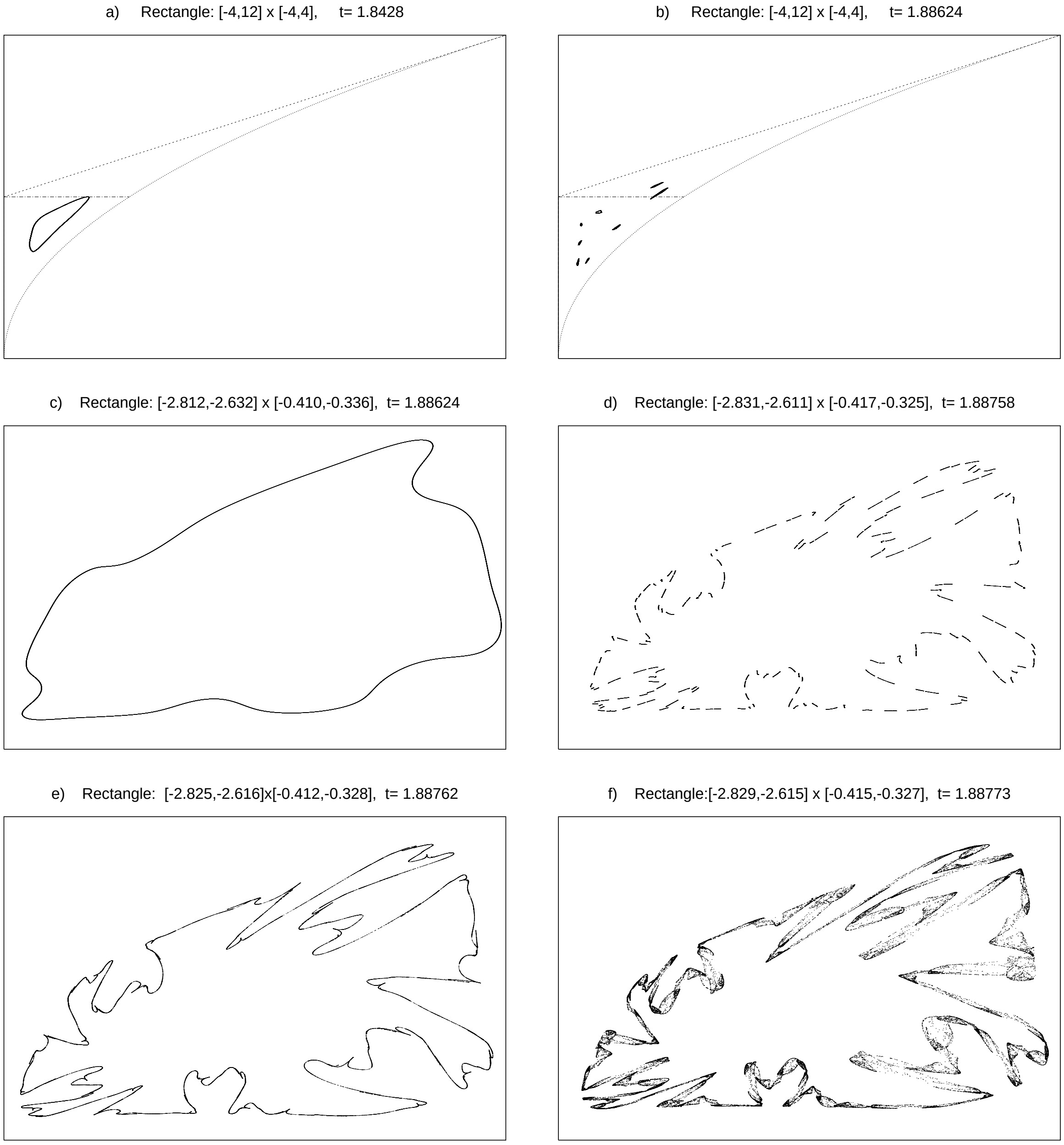

Figure 4: Attracting sets for different values of t. In Figures a) and b) we have also drawn the region R_2 and the critical line. In Figures c), d), e) and f) we have drawn the same component of the eight-pieces attractor.

the attractor collapse when the third iterate of the critical point coincides with the fixed repellor point.

Of course, it is not hard to prove the existence of a 8-periodic repellor inside the hole of the attractor for Figure 4 f) which plays the role of the fixed point for the quadratic family and takes part of the 2D attractor in Figure 5. Therefore, it is natural to expect that the inner hole of the 2D attractor disappears when some critical point belongs to the closure of the unstable set of this 8-periodic repellor. We also conjecture that, in order to capture the different attractors in all our numerical experiments, it is enough to take the forward orbit of critical points, because these orbits must design (as in the unidimensional setting) the boundary of the region in which any attractor lives.

In Figure 5, a new one-dimensional attractor can be seen. One piece (homeomorphic to a circle) of a 27-pieces attractor is shown (5 c)). This attractor will be destroyed for some slightly bigger value of the parameter due to a new Hopf bifurcation. After this Hopf bifurcation three different attractors coexist for $t = 1.88949$, see Figure 6 a). The continuation of the 2D attractor described above, the 27-periodic attractor coming from the Hopf bifurcation and a new one-dimensional attractor formed by 40 pieces. In Figure 6 b) two points of the periodic orbit are represented by crosses, and two pieces of the 1D strange attractor can be seen. This new 1D attractor rises in a already known way: There exists, for values of the parameter in $(1.88945, 1.88947)$, a 40-periodic attractor which becomes into 40 invariant circles through a Hopf bifurcation for some value of the parameter in $(1.88947, 1.88948)$. These invariant circles probably break, see once again [6], due to homoclinic bifurcations giving rise to one-dimensional strange attractors (one of the Lyapounov exponents along the 1D attractor of Figure 6 is 6.24×10^{-3}).

On the other hand, the numerically obtained Lyapounov exponents for the 2D attractor in Figure 6 are both positive and, in order to show the reliability of our numerical method for computing Lyapounov exponents we remark that the obtained exponents along the attracting periodic orbit are -1.7746×10^{-2} and -1.7749×10^{-2} (we point out that the respective periodic orbit is a focus and, therefore, the "real" Lyapounov exponents coincide).

Figure 6 c) is devoted to show the geometry (overall, it is remarkable the presence of self-intersections) of one of the pieces of the unidimensional attractor introduced in Figure 6 a), while in Figures 7 a) b) and c) we successively enlarge some region of the 2D attractor in order to confirm the presence of a periodic repellor (which is a 40-periodic focus whose eigenvalues have modulus very close to 1) and also of a 120-periodic saddle. The shape of part of the unstable set of this periodic saddle corresponds to the more marked curves ("more visited regions") in Figure 7 c). In Figure 7 d) we have drawn the invariant manifolds of the 120-periodic saddle in the same rectangle of Figure 7 c). We see inside the region determined by the unstable invariant manifold, the 40-periodic repeller focus. It is interesting to notice that this focus is near a 1:3 resonance. A study of this bifurcation, including the bifurcation diagram of the approximating flow can be found in [10].

As the parameter increases, the size of the 8-pieces 2D attractor of the previous figures grows due to the existence of inner "tongues", which will connect, for bigger values of the parameter, the eight pieces of the attractor to give rise the first 1-piece 2D attractor. In

Figure 8 a) we can see the tongues of one piece of the 8-pieces 2D attractor for $t = 1.8912$, jointly with two saddle points p and q with their invariant manifolds, that are part of a 16-periodic orbit. Moreover, in Figure 8 b) we have represented in a larger rectangle, three pieces of the 8-pieces 2D attractor, 6 points of a 16-periodic saddle and the unstable invariant manifold of one of these points, which we call p in the picture.

In Figure 9 there is a 1-piece 2D attractor with a hole, for $a = 1.892$. The merging of the 8-pieces 2D strange attractor to 1-piece is due to the birth of a heteroclinic intersection between the 8-periodic repellor inside the 8-pieces attractor and a 16-periodic expansive saddle near the 2D attractor, whose unstable invariant manifold connects the pieces of the attractor, as we can deduce from the previous figures.

The attractor given in Figure 9 is a 2D strange attractor whose numerically obtained Lyapounov exponents are both positive: 3.656×10^{-2} and 8.385×10^{-3}. Of course, in the inner hole of the attractor there exists a fixed repellor (in fact, the respective fixed point $\widetilde{P}_{a,b}$ given in (3)). Therefore, the evolution of this attractor is very similar to the one described from Figure 4 f) to Figure 5 b): A 2D attractor with an inner hole, the size of the hole decreasing as long as the parameter increases. This hole definitively disappears when some critical point belongs to the closure of the unstable set of $\widetilde{P}_{a,b}$. Nevertheless, now the whole process follows in a large set of parameters; namely, the 1-piece 2D attractor without hole does not arise until $t = 1.9302$. Moreover, in the interval of parameters $(1.892, 1.9302)$ there are other interesting situations which we must describe. Before that, we point out that the invariant measure associated to the 2D attractor in Figure 9 concentrates at eight pieces of the attractor. This is due to the existence, for slightly smaller values of t, of the 8-pieces strange attractor plotted in Figure 8 a). In Figure 9 we may distinguish the shape of one of these pieces and even how its inner "tongues", which have been described above, "leave" this 2D marked region.

The 2D strange attractor appearing in Figure 9 vanishes due to local bifurcations: Some periodic point becomes an attractor for some parameter in $(1.89276, 1.89278)$. Furthermore, along the range of parameters $(1.89278, 1.89992)$ many already described bifurcations take place: There exists an 11- periodic attracting orbit which is transformed through a Hopf bifurcation into a 11-circles 1D attractor. This attractor follows the bifurcation scheme announced in [6]: The one-dimensional attractor formed by circles are close enough to periodic saddles whose invariant sets collapse and these homoclinic or heteroclinic bifurcations bring out the appearance of chaotic attractors. At the same time, the same holds for a 22-pieces attractor which, for some open set of parameters coexists with the above one. However, this new attractor experiments the same sequence of bifurcations described for the 11-pieces attractor, but in inverted sense: As the parameter increases this 22-pieces attractor evolves from a chaotic attractor to a periodic one. Let us illustrate these parallel processes followed by these two attractors with several numerical experiments.

In Figure 10 a) we may see the global layout in R_2 of these two attractors for $t = 1.898$. By making a magnification near the critical line, see Figure 10 b), we distinguish one piece of the 1D attractor, which is homeomorphic to a circle, and two pieces of the 2D attractor. On this 2D attractor the obtained exponents are 1.347×10^{-3} and -2.833×10^{-2}. Hence, this 2D strange attractor is already quite "weak" (the sum of the Lyapounov exponents

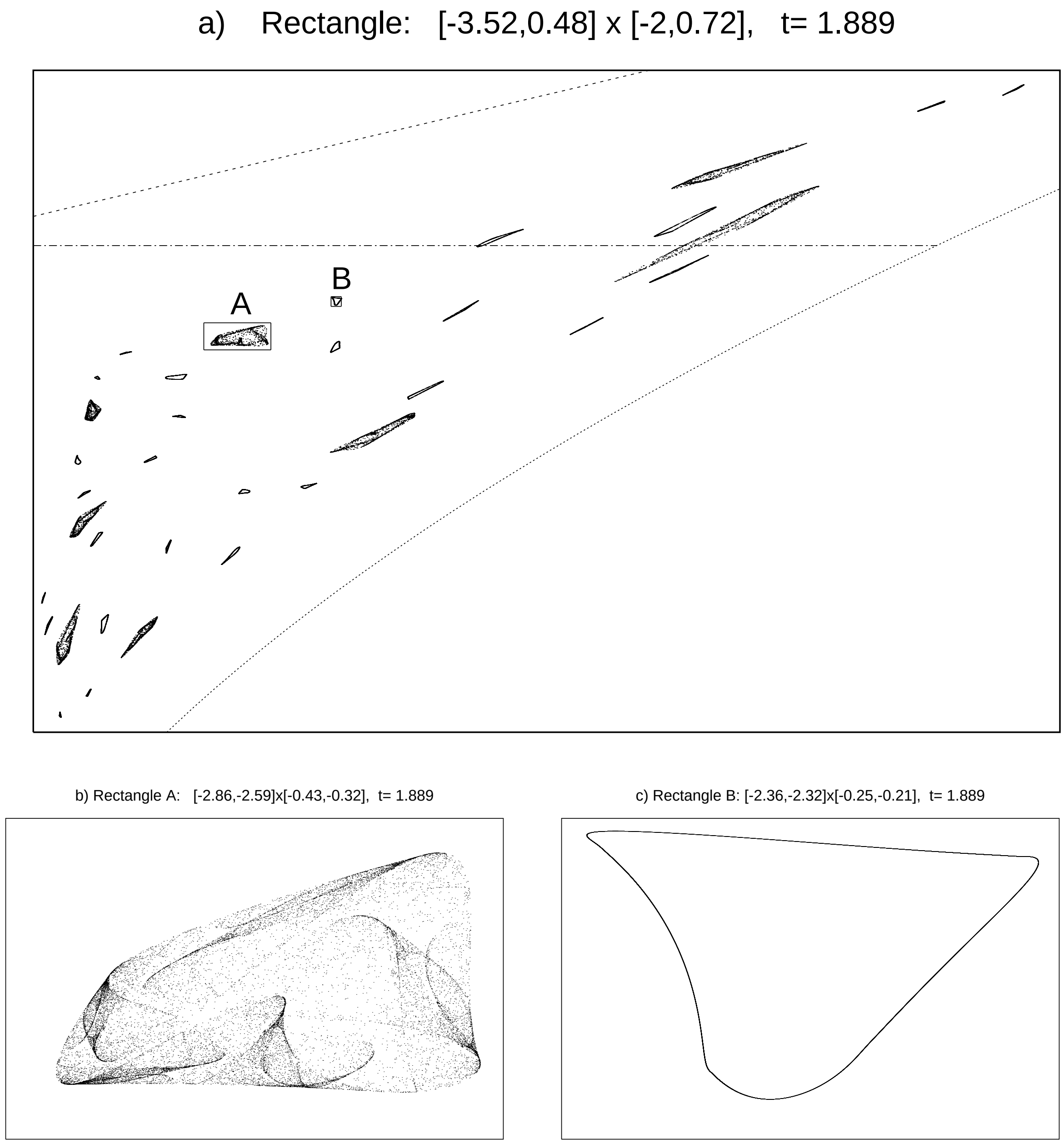

Figure 5: Attracting sets for $t = 1.889$. The figures b) and c) are, respectively, magnifications of one piece of the two-dimensional attractor and the IC.

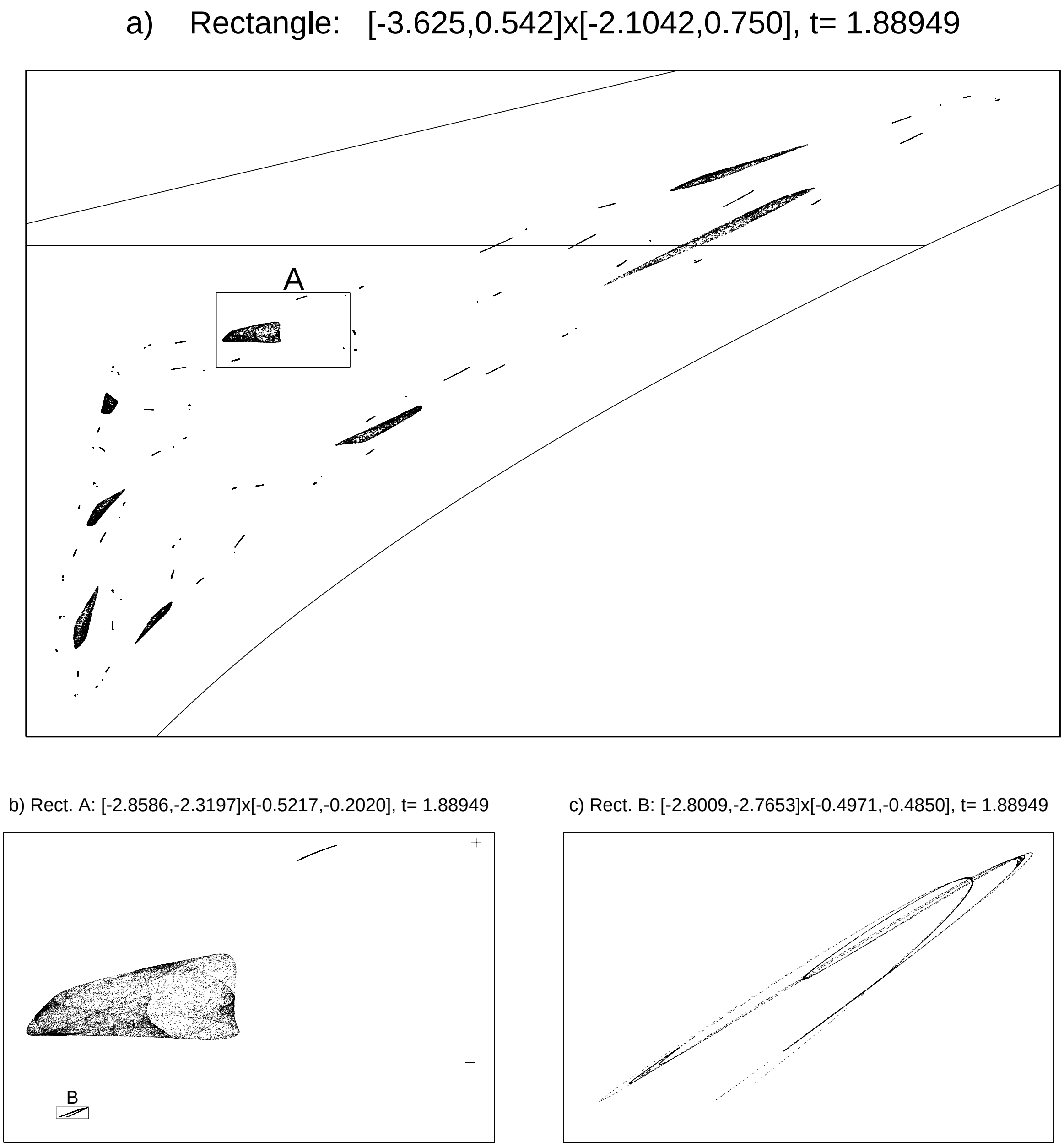

Figure 6: Attracting sets for $t = 1.88949$. Figure b) is a magnification of the rectangle A. The two crosses appearing in this window represent two iterates of a 27-periodic attractor. Figure c) is a magnification of the rectangle B.

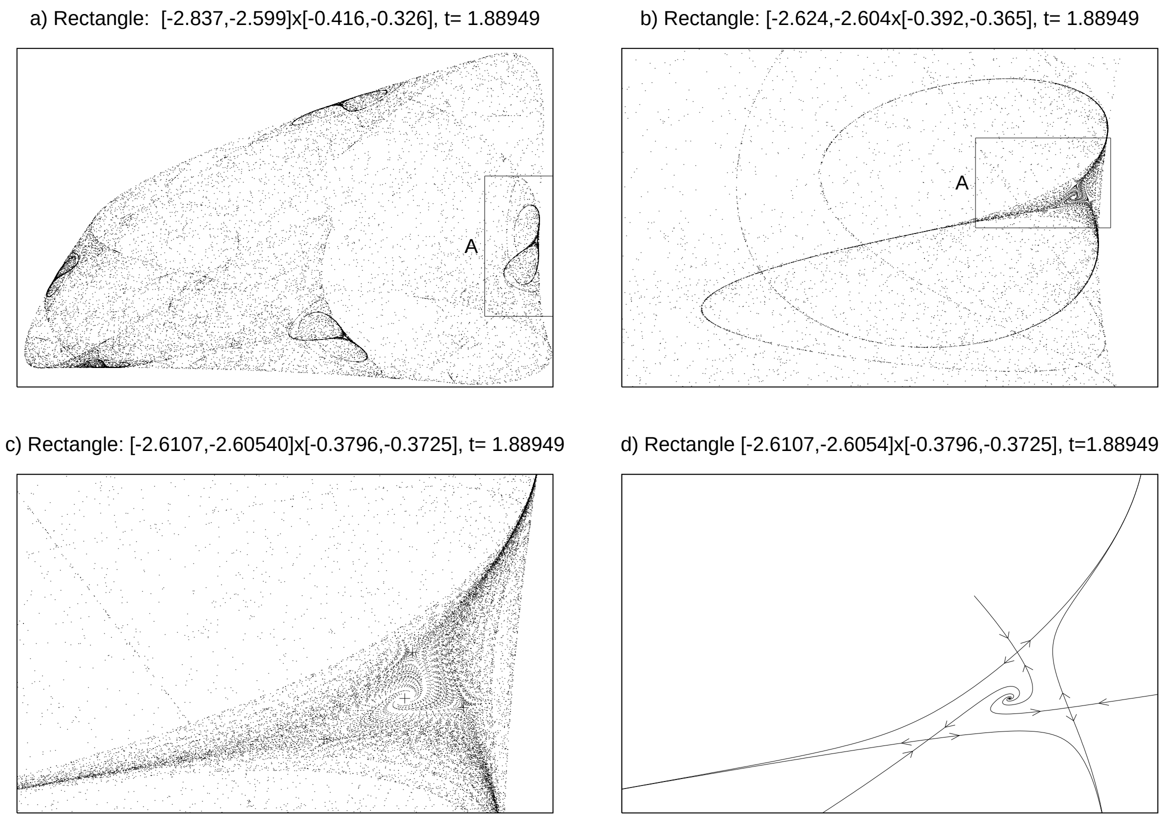

Figure 7: Left up: Magnification of the 2D attracting set of Figure 6 b). Right up: Magnification of the rectangle A of the previous figure. Down left: Magnification of the rectangle A of the previous figure. Down right: The same rectangle of the previous figure, with the invariant manifolds of the 120-periodic saddle.

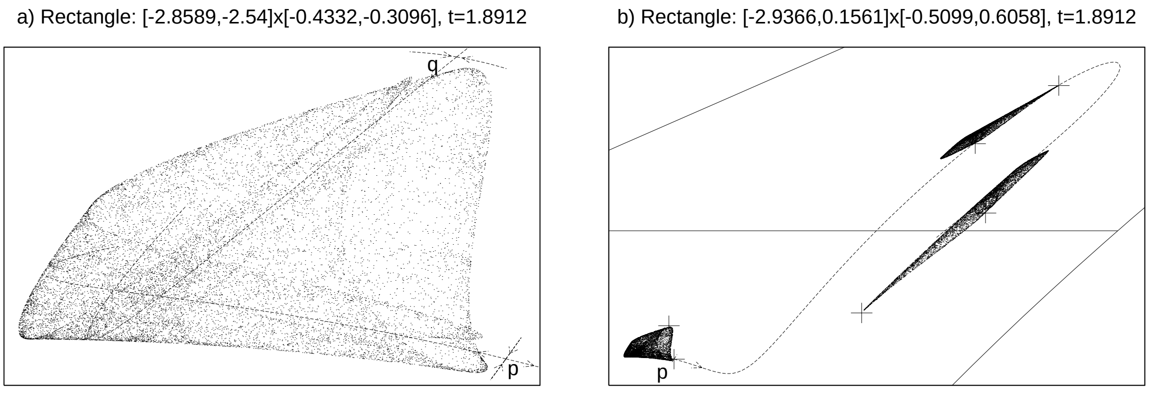

Figure 8: a) A piece of a 8-pieces 2D attractor with "tongues" and two iterates of a 16-periodic saddle jointly with their invariant manifolds. b) Three of the pieces of the 8-pieces attractor, jointly with 6 iterates of a 16-periodic saddle, represented by crosses. Moreover, the unstable invariant manifold of the point p is included.

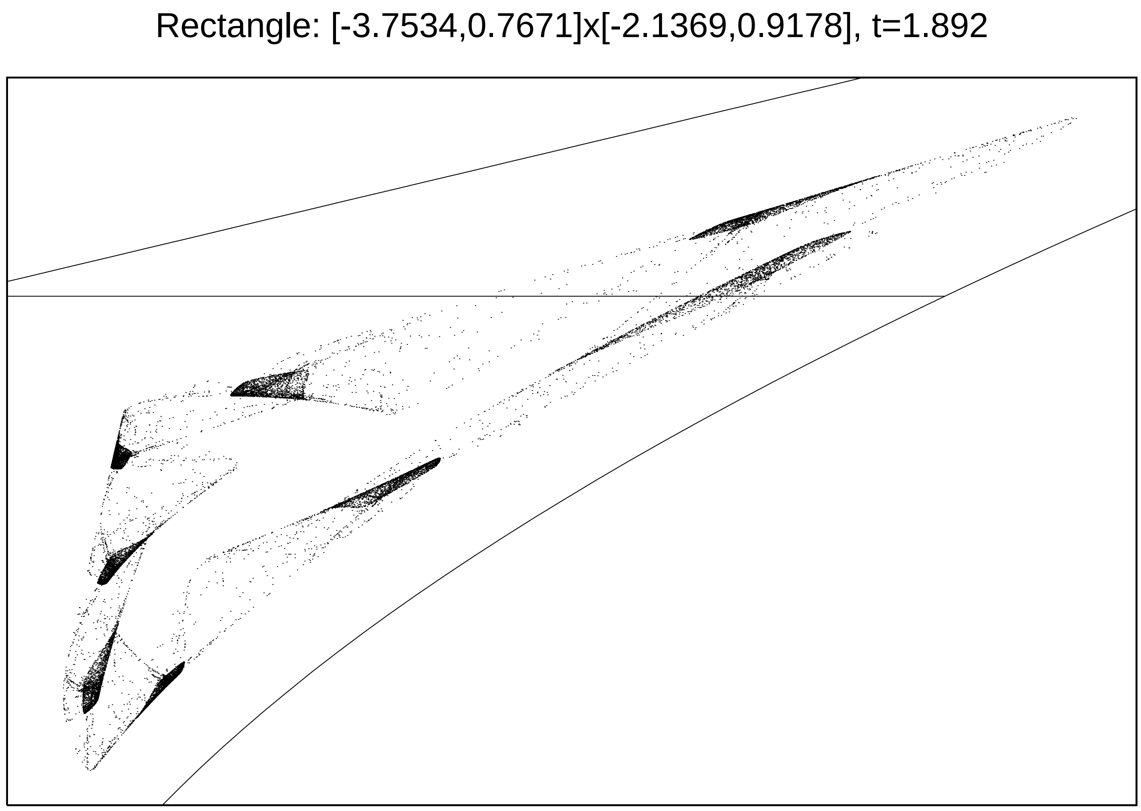

Figure 9: A 1-piece 2D strange attractor.

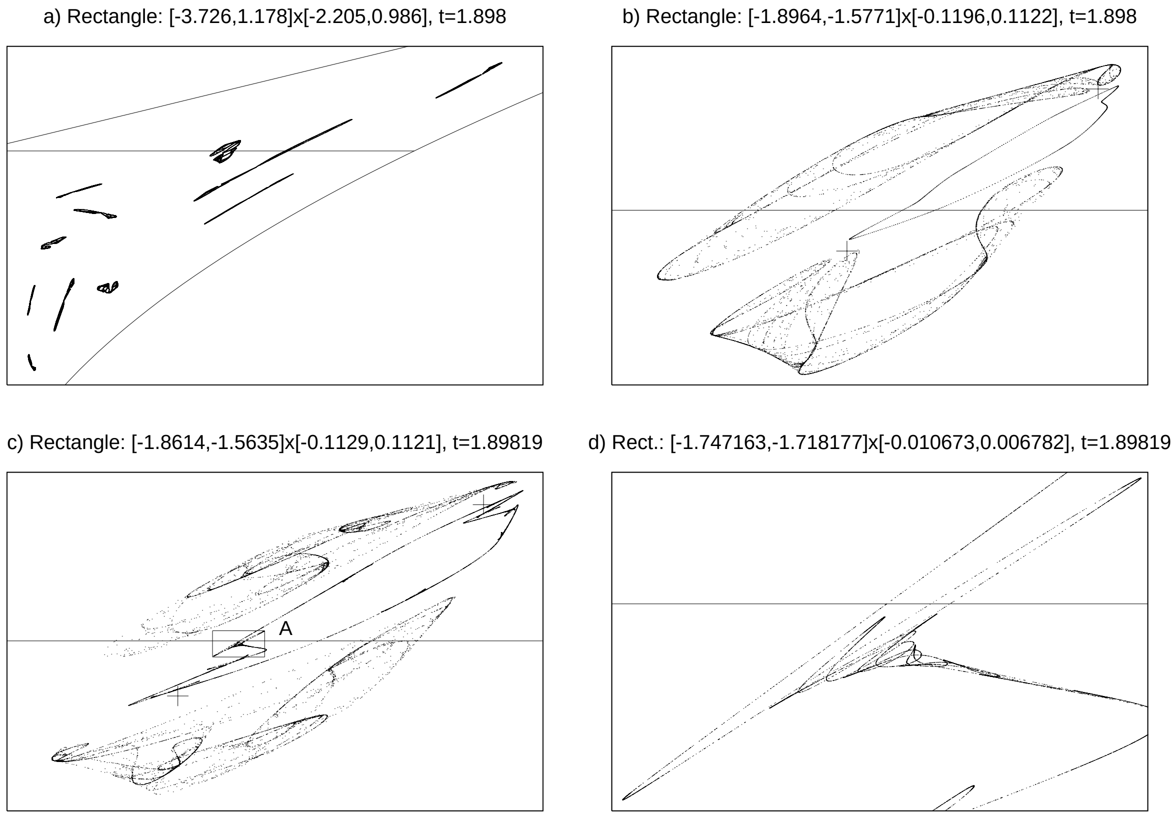

Figure 10: Several attractors inside the region R_2. The critical line and the boundary of R_2 are included and the crosses are periodic points of period 22. Figure b) is a magnification of a) and d) is a magnification of rectangle A in Figure c).

is far from being positive). A numerical analysis also allows us to detect, very close to both attractors, a 22-periodic expanding saddle (the product of its eigenvalues is bigger that one) which is the candidate to produce chaotic attractors from the unidimensional one. In Figure 10 c), two points of this 22-periodic orbit are represented by crosses.

As was expected, for slightly large values of the parameter the 1D attractor is no longer homeomorphic to circles, see Figure 10 c) in which both attractors are represented for $t = 1.89819$. The one-dimensional attractor exhibits loops and cusps according to the magnification made in Figure 10 d). This situation is, once again, the prelude to the birth of chaotic 2D attractors instead of 1D attractors. For this value of the parameter the 1D attractor already presents a positive Lyapounov exponent.

After homoclinic or heteroclinic bifurcations, the continuations of these two attractors are shown in Figure 11 a) for $t = 1.898244$. The previous 1D attractor breaks into several pieces, one of them represented in the next picture, see Figure 11 b). In fact, it seems to be a unidimensional set with self-intersections which probably arises in the vicinity of homoclinic orbits associated to a 198-periodic saddle, represented in this figure by a cross. For both attractors in Figure 11 a), one of the Lyapounov exponents is positive and the other one is negative.

In order to follow the competition between these two different attractors one may repeat the numerical experiments from Figure 10 a) to Figure 11 a), by taking twenty initial conditions uniformly distributed on the critical line. It is remarkable that, in Figure 10 a) the 1D attractor only captures three of these twenty orbits (the remainder travel to the 2D attractor) while for the situation given in Figure 11 a) thirteen initial conditions go the 2D attractor and seven do to the unidimensional one.

In fact, for $t = 1.89827$ (see Figure 11 c)) the 22-pieces attractor decomposes into 12×22 unidimensional pieces, while the 11-pieces attractor transforms into a 11-pieces bidimensional attractor. Both of them have a Lyapounov exponent of each sign, but for the 11-pieces 2D strange attractor the sum of the exponents becomes positive. We note that for a previous 198-periodic saddle for $t = 1.89819$ inside this attractor becomes a repellor and a 99-periodic expansive saddle is born by a saddle-node bifurcation. After new homoclinic or heteroclinic bifurcations the 22-pieces attractor turns homeomorphic to circles, according to Figure 11 d) ($t = 1.898884$). Inside these circles one can find a 22-periodic repelling focus near a Hopf bifurcation. The size of the 11-pieces attractor grows (and also the sum of its Lyapounov exponents) and now, it look likes a 2D attractor with a hole. We have include in the corresponding figure, part of a 99-periodic expanding saddle. It can be seen that all these saddle points have heteroclinic intersections with the neighbour one. Hence, the transition of this attractor is known.

For $t = 1.89919$, see Figure 11 e), there only exists one attractor, which is the continuation of the previous 11-pieces 2D strange attractor, but now with 5×11 2D pieces. The other one disappears once a new Hopf bifurcation and a new saddle-node bifurcation take place. It is interesting to note that in this case inside all the pieces there is a 55-periodic slightly dissipative saddle. It seems that the closure of its unstable invariant manifold is a 2D set, because the sum of the Lyapounov exponents of the attractor are positive but small.

For $t = 1.8992$, see Figure 11 f), there only exists one attractor: The continuation of the 5×11-pieces 2D strange attractor described before, which is now again a 11-pieces attractor due to the appearence of homoclinic and heteroclinic bifurcations. We again observe the existence of "tongues" inside the 2D attractor. These "tongues" will be, once again, the cause of the appearance of a global 1-piece 2D attractor, see Figure 12 a) for $t = 1.9$, like the one studied in Figure 9. We point out that this evolution was already discovered before (see Figure 9). The shape of the attractors giving rise to the 1-piece 2D one is quite similar in both cases: Bidimensional pieces with "leaving tongues". The only difference in the last case is that we have not found a previous heteroclinic bifurcation with an expanding saddle before the homoclinic bifurcation of the repelling periodic saddle inside the 11-pieces attractor.

The size of the attractor showed in 12 a) is bigger than the size of the one obtained in 9. This common phenomenon for passing from 2D attractors with inner holes to 2D attractors without holes was observed several times along the numerical analysis for 2D attractors. In any way, before the 2D 1-piece global attractor without holes arises, new local bifurcations of periodic points for some value of the parameter in $(1.90012, 1.900123)$ bring about the appearance of a 44-pieces attractor. See Figure 12 b) to check the global arrangement of this attractor for $t = 1.900123$, and also Figure 12 c) in which one of its

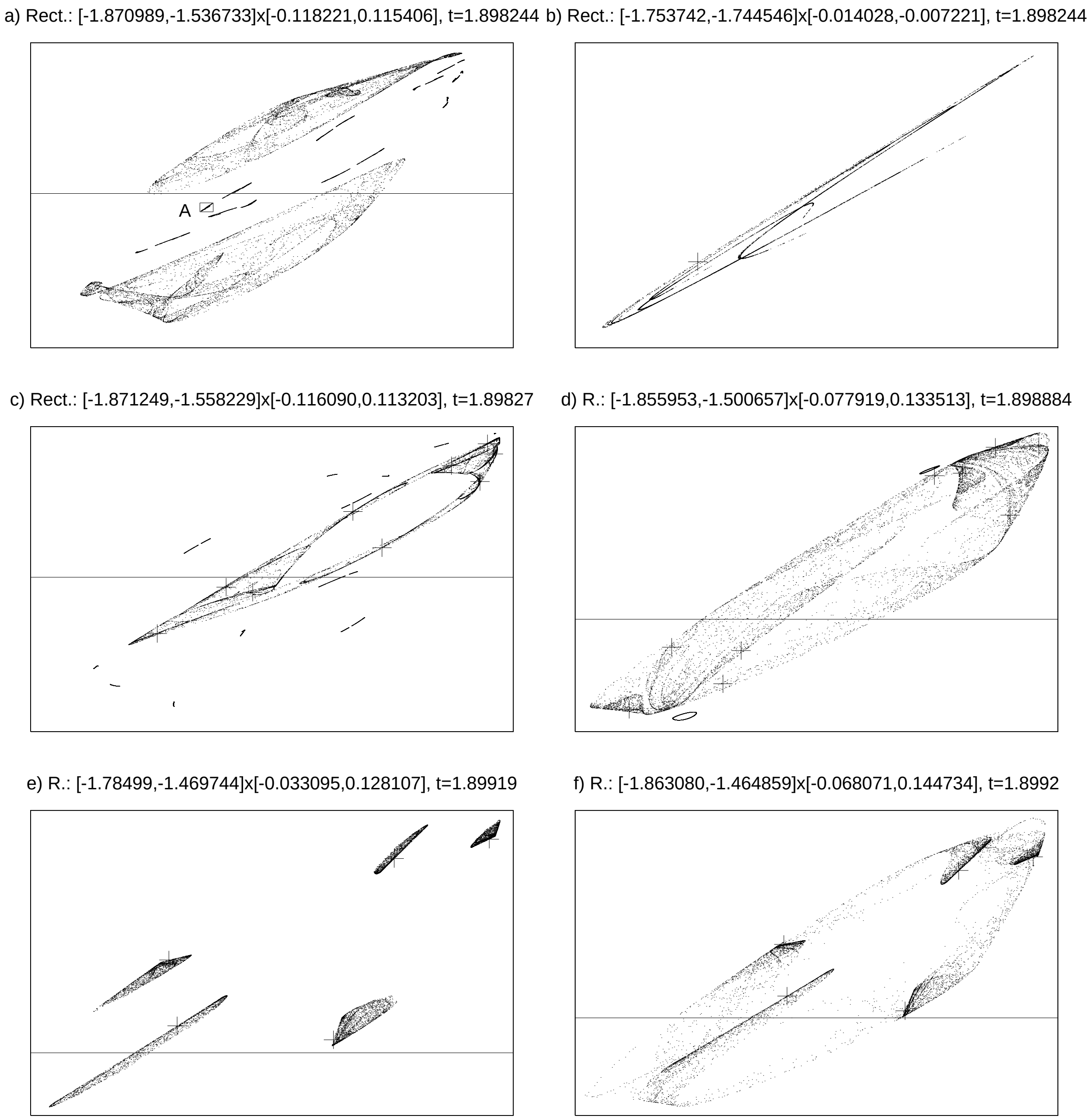

Figure 11: a) Evolution of the attractors of Figure 10. Figure b) is a magnification of the rectangle A of a). The cross indicates the existence of a 198-periodic saddle. In Figure c) part of a 99-periodic expansive saddle is marked with crosses. In Figure d), the crosses are again part of a 99-periodic expanding saddle. In Figures e) and f) the crosses are 55-periodic saddles.

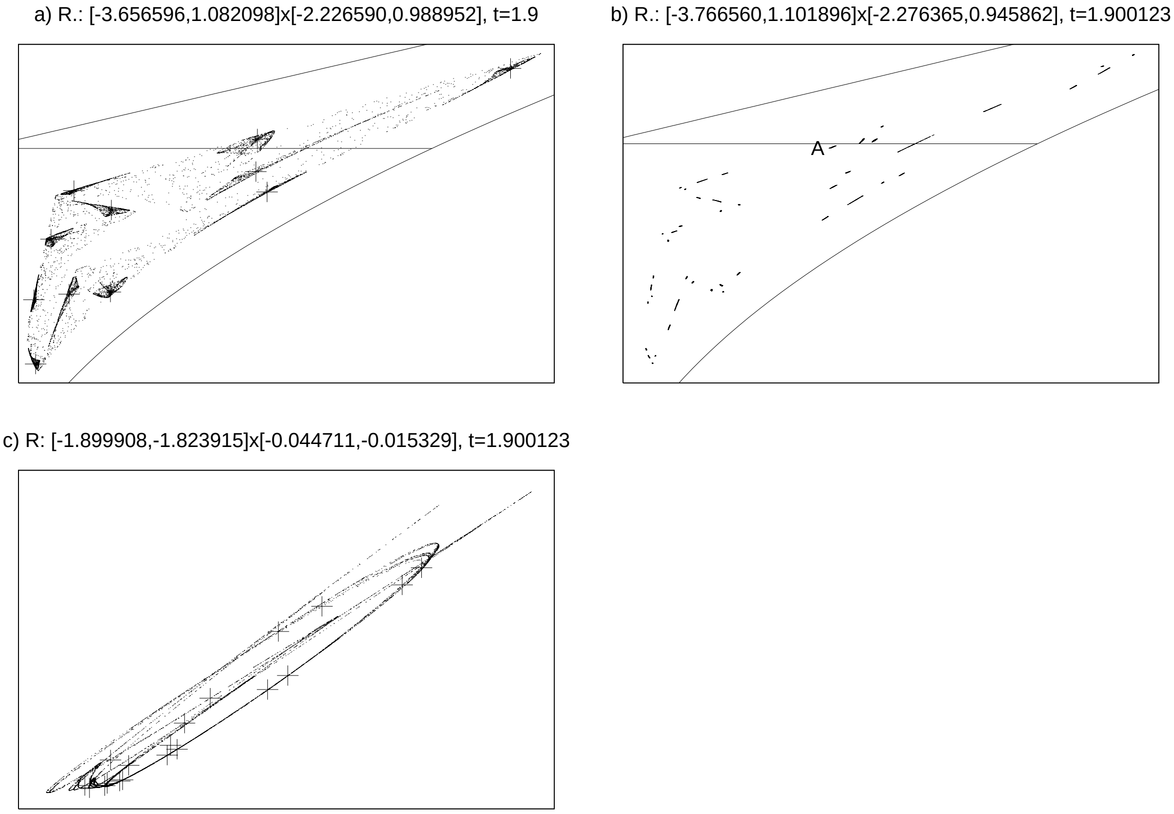

Figure 12: a) 1-piece 2D strange attractor. The crosses indicate points of a repelling focus of period 11. b) Evolution of the previous attractor. c) Magnification of the piece A of the 44-periodic attractor of the previous figure. The crosses indicate periodic points. See the explanation in the text.

pieces is represented. In this case one of the Lyapounov exponents is positive although the sum of both exponents is negative. Moreover in this last picture we have drawn two iterates of a 396 ($= 9 \times 44$) periodic saddle in the attractor, and one 44-periodic repelling focus in the hole inside the attractor.

Let us point out that by taking 10^4 equidistant parameters in the set $(1.9, 2)$, most of the obtained situations have been already observed for certain windows in the domain of parameters $(1.8, 1.9)$. Hence, let us finish this section by introducing not only those numerical experiments which seem to offer new kinds of attractors, but also those ones which may clarify some of the previously explained bifurcations. For instance, for $t = 1.901208194$ we have a 36–pieces 2D strange attractor with a hole inside every piece. In Figure 13 a) we have drawn one of the pieces of this attractor. We note that sorrounding the hole in this attractor, there exists a triangular region where there is more density of points of the attractor. Near each vertex of this triangle one iterate of a 108 (3×36) expanding periodic saddle is located, whose unstable invariant manifold is contained in the attractor. We have also drawn a point inside the hole that belongs to a repelling focus of period 36. Changing slightly the parameter ($t = 1.901208196$) we see that the 36-pieces attractor now is a thick triangle, and the rest has disappeared. This is because for some intermediate t the map has undergone a heteroclinic tangency between the unstable invariant manifold of some saddle in the thick triangle and the stable invariant manifold of the 108-periodic saddle near the vertices of the triangle (see Figure 13 b)). For $t = 1.90120842$, a 108-pieces 2D strange attractor and a 36-pieces attracting invariant curve with triangular shape, coexist (see Figure 13 c)). The 2D attractor is destroyed when a heteroclinic intersection between the stable invariant manifold of the 108-periodic saddle near the vertices of the triangular invariant curve, and the unstable invariant manifold of some 108-periodic repellor inside the 2D attractor, takes place for a slightly small value of t. In Figure 13 d) there is a magnification of Figure c), where the invariant manifolds of one of the saddle points are drawn.

In Figure 14 a) we present a new class of attractor for $t = 1.9379$. Since the obtained exponents are 0.130 and -0.078 we are dealing with an expanding map for which is noteworthy the size of the positive Lyapounov exponent. In spite of several windows of periodic sinks, this attractor is born from the already mentioned global 1-piece 2D attractor without holes. The respective bifurcation probably takes place due to heteroclinic bifurcations between the invariant manifolds of periodic points. In fact, one may numerically detect a 3-periodic expanding saddle inside the attractor and also a 3-periodic repelling node. The attractor must corresponds to the closure of the unstable set of the 3-periodic expanding saddle and must be contained in the unstable invariant set of the repelling node. In Figure 14 b) we have drawn a magnification of one of the pieces of the strange attractor.

The fact that the attractor in Figure 14 coincides with the closure of the unstable manifold of a expanding periodic orbit with real eigenvalues probably explains the fact that its geometry was substantially different than the one exhibited by the previously obtained several-pieces 2D attractors: These last ones always seem to correspond to the unstable set of repelling periodic foci. In any case, the future evolution of the attractor in Figure 14 was already observed: As the parameter increases the size of its pieces

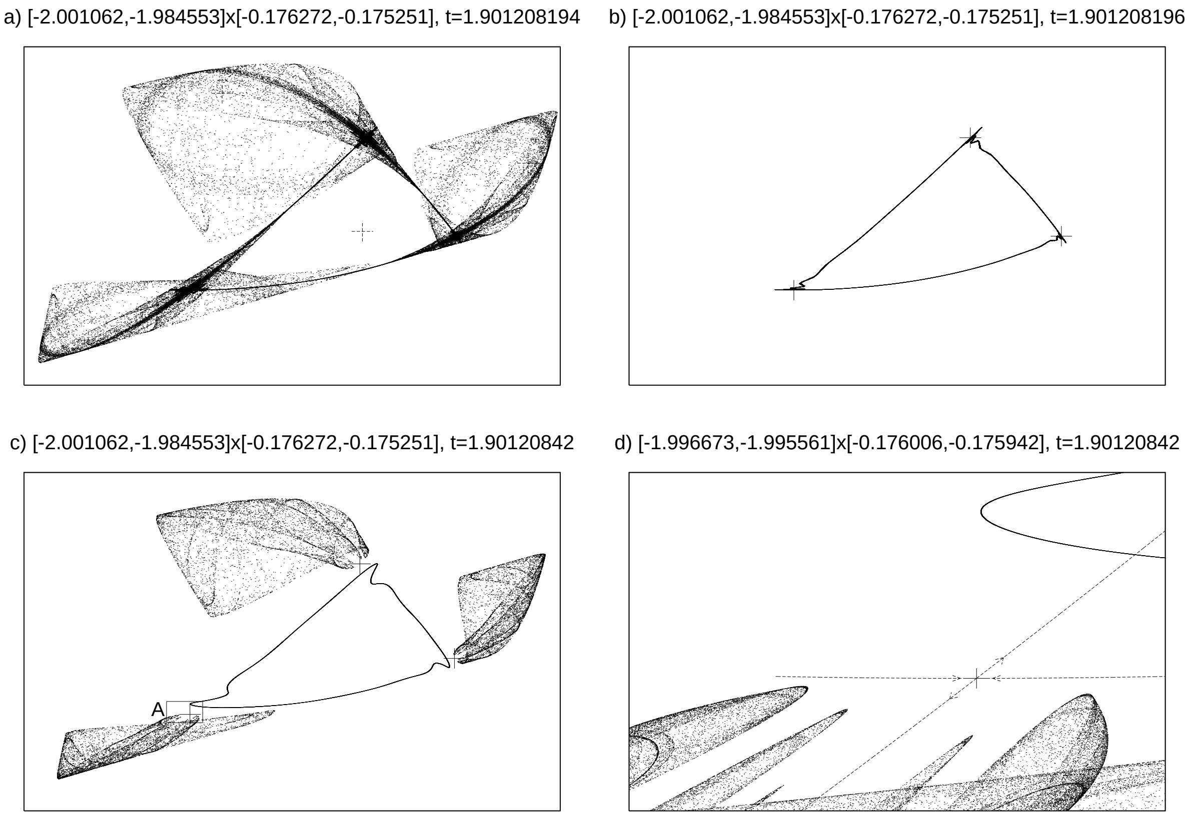

Figure 13: a) One piece of a 36-pieces 2D strange attractor. The cross indicates a point of a repelling focus of period 36. b) One piece of a 36-pieces 1D strange attractor. The crosses indicate points of a 108-periodic saddle. c) Three pieces of a 108-pieces 2D strange attractor, one piece of a 36-pieces attracting invariant curve, and three points of a 108-periodic saddle. d) Magnification of the rectangle A of the previous figure. The invariant manifolds of the saddle are drawn.

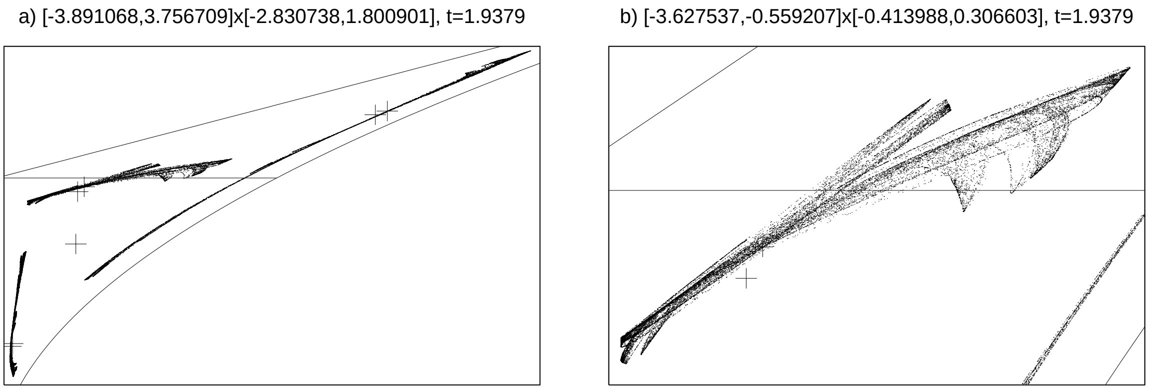

Figure 14: a) A 3-pieces 2D strange attractor. The crosses inside the attractor represent a period three expanding saddle, and near this periodic saddle, it is also represented a 3-periodic expanding node near, but outside the attractor. The cross on the central part of the picture is a repelling 1-periodic focus. b) Magnification of one of the pieces of the attractor.

grows until a new global heteroclinic bifurcation (interaction with the stable set of the 1-periodic repelling focus (see the cross in the central part of Figure 14 a)) produces the new apparition of the 1-piece 2D global attractor without holes for certain value in the range of parameters $(1.944, 1.95)$.

The first five pictures in Figure 15 are devoted to explore a new global bifurcation. The process starts in Figures 15 a) and b) where a 32-pieces 1D strange attractor emerges for $t = 1.97981$. In Figure 15 b) eight of these pieces are displayed (inside each piece we have represented with a cross a 32-periodic dissipative saddle). Each one of them seems to be a Hénon-like strange attractor associated to the displayed dissipative saddle, which probably shows up from a heteroclinic or homoclinic bifurcation. In fact, several expanding and dissipative saddle periodic points are found in the set of parameters $(1.97981, 1.97987)$ close to the respective attractor.

The pieces of the attractor in Figure 15 b) collapse two by two to form a 16-pieces 2D strange attractor for $t \approx 1.979814$. In Figure 15 c) one piece of this new attractor can be seen. The Lyapounov exponents for this value of the parameter are 0.0209 and -0.0247. We have drawn also two points of a 32-periodic weakly expansive saddle, whose unstable invariant manifold generated the previous 32-pieces 1D strange attractor, two points of a 32-periodic expanding saddle and one point of a 16-periodic repelling node outside the attractor. Nevertheless, the presence of repelling nodes, expanding saddles and the possible interactions between their invariant manifolds would be very relevant in order not only to justify the complicated geometry of these attractors but also to understand what kind of bifurcations lead to them. In Figure 15 d) we have represented the invariant manifolds of the 32-periodic points of the previous figure. We notice that $W^u(C)$ and $W^u(D)$ have intersections with $W^s(A)$ and $W^s(B)$. Moreover, $W^u(A)$ and $W^s(C)$ have an intersection that is near to be tangent. This is also the case of $W^u(B)$ and $W^s(D)$. All these heteroclinic intersections explain why the 32-pieces attractor has become a 16-pieces attractor. Finally, we notice that points C and D has been born by a flip bifurcation of the point E.

In Figure 15 e) we may see the continuation of one piece of the above 16-pieces attractor for $t = 1.97983$. The sum of the Lyapounov exponents has grown (and is positive). Moreover, the hole inside the attractor has disappeared. This is because one of the saddles has become a repelling node, and the unstable invariant manifold of this node has intersections with the stable invariant manifold of the 16-periodic repelling node. If $t = 1.97987$ the whole attractor has four pieces (once again, several pieces of the old attractor collapse probably due to heteroclinic bifurcations) with a hole, where there is a 4-periodic repelling focus, similar to other previous cases. Repelling periodic nodes and expanding periodic saddles for this value of the parameter are also detected, and we note that the Lyapounov exponents of the attractor are both positive.

Finally, in Figure 15 f) the obtained attractor is shown for $t = 1.99999$. As was conjectured, see Conjecture 10, this situation would be frequently (with positive probability) observed for values of the parameter sufficiently close to $t = 2$: All the invariant set R_2 is a 2D strange attractor with two positive Lyapounov exponents. For this particular value of the parameter the obtained exponents are 0.344 and 0.343, which are, as was also expected, very close to the value $\frac{1}{2}\log 2$, the (both) Lyapounov exponents for the bidimensional tent map studied in Section 2. Furthermore, by making 10^3 equidistant experiments in the range of parameters $(1.99, 2)$ the shape of the obtained attractor always coincides with the whole domain R_2. Of course, this is not a proof of Conjecture 10.

4 Conclusions

We have studied a two-parameter family of quadratic non-invertible two-dimensional maps which are limit return maps associated to some type of codimension-two homoclinic tangencies in dimension three. We have proved that this family has two-dimensional strange attractors, including one case in which the map is completely uncoupled (see Section 2). Moreover, we have chosen a one-parameter family (contained in the original two-parameter family) for which we have performed numerical computations in order to find its attractors. We have found that many kinds of attractors (periodic orbits, closed invariant curves and strange attractors of dimensions one and two) can coexist. Moreover, we have detected a mechanism to create two-dimensional strange attractor from attracting invariant curves, that seems to be very common in these class of maps. The process can be described in the following way:

Suppose that for certain value of the parameter there exists an attracting invariant curve. This curve can be destroyed by several mechanism. When the map is dissipative in a neighbourhood of the invariant curve, these mechanisms have been described in [3]: The appearence of a flip bifurcation of some periodic attractor inside the invariant curve, or the presence of some homoclinic or heteroclinic bifurcations of some of its saddles. In the first case only attracting periodic orbits persist and in the second case, one-dimensional strange attractors are born. If one of these dissipative saddles transform into an expansive one, then these 1D attractors become two-dimensional ones. Later, due to more homoclinic and/or heteroclinic intersections it is possible that these 2-D attractors, which can have many pieces, merge to a one piece 2D-strange attractor which can have an annular form, resembling the initial invariant curve, or a 2D object without holes. When the initial invariant curve is not dissipative, another phenomenon can destroy the curve: The appearance of a Hopf bifurcation of some of its periodic points. Then, the invariant curve is replaced by an attractor consisting of several closed curves (a periodic invariant curve). After this bifurcation, we can find the same phenomenon for the small invariant curves, or the phenomenon previously described.

Finally, we want to stress that an invariant object can be destroyed by the 'collision' with another invariant object, or more specifically, by heteroclinic intersections, as we also have seen in our simulations.

Acknowledgements

We are indebted to C. Simó for fruitful discussions and suggestions. This work has been partially supported by FICYT project number PB-EXP01-29, DGES project PB98-1074, MCyT grants MCT-02-BFM-00241 and BFM2003-09504-C02-01, and CIRIT grant 2001SGR-70.

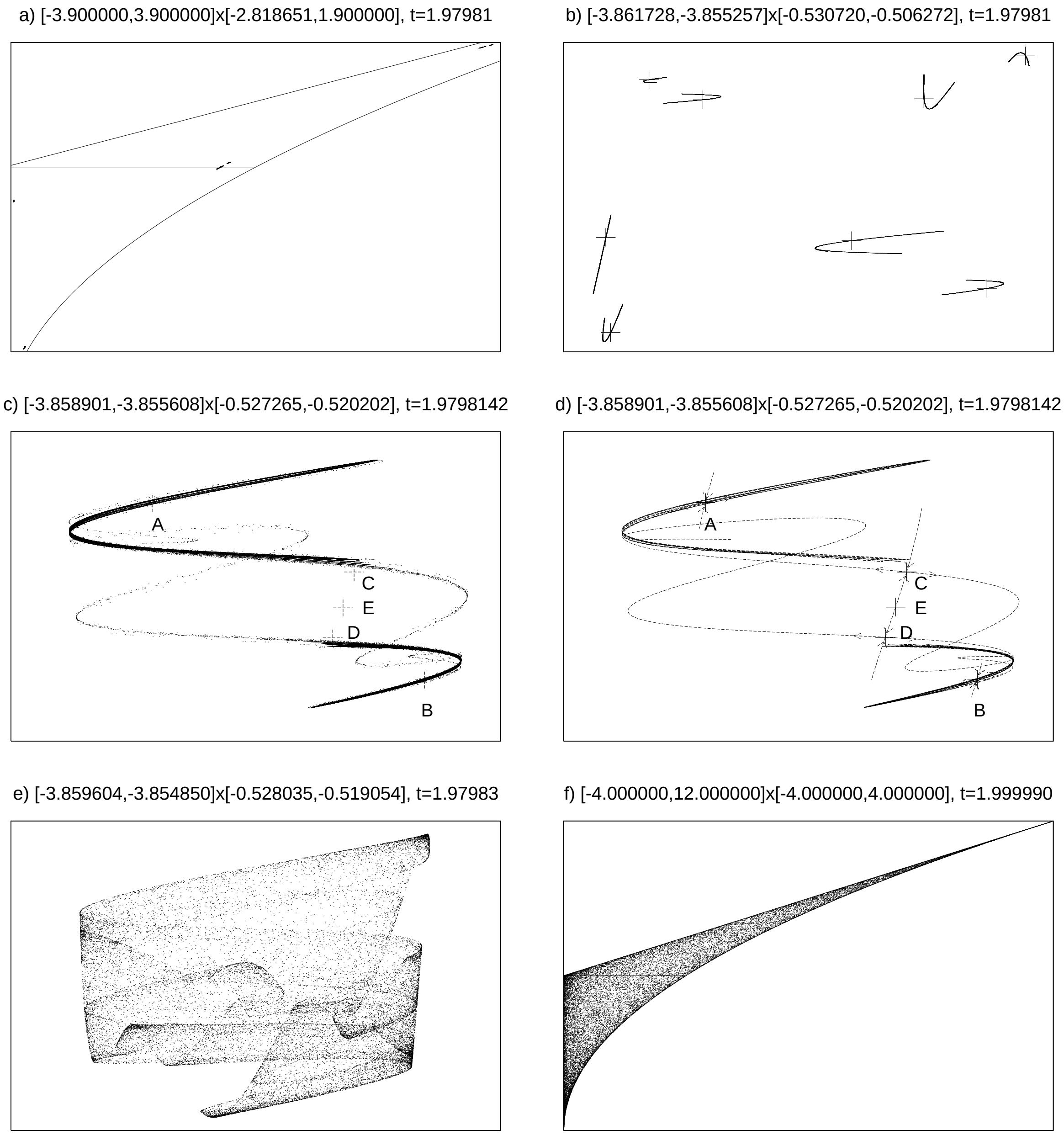

Figure 15: a) A 16-pieces 1D strange attractor. b) Magnification of eight pieces of the previous figure. c) One piece of a 16-pieces 1D strange attractor. The points A and B belongs to a 32-periodic dissipative saddle, C and D to a 32-periodic expanding saddle and E to a 16-periodic repelling node. d) The same parameter t and the same rectangle of the previous figure with the invariant manifolds of the previous periodic points. e) Evolution of the same piece of the previous attractor for $t = 1.97983$. f) A global attractor for $t = 1.99999$.

References

[1] **M. Benedicks, L. Carleson**. *On iterations of 1-ax^2 on* $(-1, 1)$. Ann. Math. **122** (1985), 1-25.

[2] **M. Benedicks, L. Carleson**. *The dynamics of the Hénon map.* Ann. Math. **133** (1991), 73-169.

[3] **H. Broer, C. Simó, J. C. Tatjer**. *Towards global models near homoclinic tangencies of dissipative diffeomorphisms.* Nonlinearity **11** (1998), 667-770.

[4] **P. Collet, J.–P. Eckmann**. *Iterated maps of the interval as Dynamical Systems.* Birkhauser, Boston (1980).

[5] **C. E. Frouzakis, L. Gardini, I. G. Kevrekidis, G. Millerioux, C. Mira**. *On some properties of invariant sets of two-dimensional noninvertible maps.* Int. Jour. Bifur. and Chaos **7** (6) (1997).

[6] **C. E. Frouzakis, I. G. Kevrekidis, B. B. Peckham**. *A route to computational chaos revisited: noninvertibility and the breakup of an invariant circle.* Physica D **177** (2003), 101-121.

[7] **S. V. Gonchenko, V. S. Gonchenko, J. C. Tatjer**. *Bifurcations of three-dimensional diffeomorphisms with non-simple quadratic homoclinic tangencies and generalized Hénon maps.* Math. Preprint Series, Universitat de Barcelona **366**. Dec. 2004.

[8] **S. V. Gonchenko, D. V. Turaev, L. P. Shil'nikov** *On the dynamic properties of diffeomorphisms with homoclinic tangencies.* J. Math. Sci. (N. Y.) **126** (2005), 1317–1343.

[9] **M. Jacobson**. *Absolutely continuous invariant measures for one parameter families of one-dimensional maps.* Commum. Math. Phys. **81** (1981), 39-88.

[10] **Y. A. Kuznetsov**. *Elements of Applied Bifurcation Theory.* Second Edition. Springer-Verlag, New York (1998).

[11] **E. N. Lorenz**. *Computational chaos-a prelude to computational instability.* Physica D **35** (1989), 299-317.

[12] **R. Mañé**. *Ergodic Theory and Differentiable Dynamics.* Ergebnisse der Mathematik und ihrer Grenzgebiete, vol. 8. Springer, Berlin (1987).

[13] **W. de Melo, S. van Strien**. *One-dimensional dynamics.* Springer-Verlag (Berlin) (1993).

[14] **C. Mira, L. Gardini, A. Barugola, J. C. Cathala**. *Chaotic dynamics in two-dimensional noninvertible maps.* World Scientific, Singapore (1996).

[15] **L. Mora, M. Viana**. *Abundance of strange attractors.* Acta Mathematica **171** (1993), 1-71.

[16] **J. Palis, F. Takens**. *Hyperbolicity & sensitive chaotic dynamics at homoclinic bifurcations.* Cambridge Studies in Advanced Mathematics **35**, Cambridge University Press (1993).

[17] **J. Palis, M. Viana**. *High dimension diffeomorphisms displaying infinitely many sinks.* Ann. Math. **140** (1994), 91-136.

[18] **H. Poincaré**. *Sur le problème des trois corps et les équations de dynamique (Mem. couronné du prix de S.M. le roi Oscar II de Suède).* Acta Math. **13** (1890), 1-270.

[19] **A. Pumariño, J. A. Rodríguez**. *Coexistence and persistence of strange attractors.* Lecture Notes in Mathematics **1658**, Springer (1997).

[20] **A. Pumariño, J. A. Rodríguez.** *Coexistence and persistence of infinitely many strange attractors.* Ergodic Theory and Dynamical Systems **21** (2001), 1511-1523.

[21] **A. Pumariño, J. C. Tatjer.** *A possible new family of two dimensional strange attractors.* In F. Dumortier, H. Broer, J. Mawhin, A. Vanderbauwhede, and S. Verduyn Lunel, editors, *International Conference on Differential Equations* (Equadiff 2003), pages 434–439. Held in Hasselt (Belgium), 22-26 July, 2003. World Scientific, Singapore, 2005.

[22] **R. Rico-Martínez, R. A. Adomaitis, I. G. Kevrekidis**. *Non-invertibility in neutral networks.* Computers and Chemical Engineering **24** (2000), 2417-2433.

[23] **J. C. Tatjer, C. Simó**. *Basins of attraction near homoclinic tangnecies.* Ergodic Theory and Dynamical Systems **14** (1994), 351-390.

[24] **J. C. Tatjer**. *Three-dimensional dissipative diffeomorphisms with homoclinic tangencies.* Ergodic Theory and Dynamical Systems **21** (2001), 249-302.

[25] **M. Viana**. *Strange attractors in higher dimensions.* Bol. Soc. Bras. Mat. **24**, (1993), 13-62.

[26] **M. Viana**. *Multidimensional nonhyperbolic attractors.* Inst. Hautes Etudes Sci. Publ. Math. **85** (1997), 63-96.

[27] **P. Walters**. *An Introduction to Ergodic Theory.* Graduate Texts in Math., vol. 79. Springer, Berlin (1982).

[28] **L.-S. Young**. *Decay of correlations for certain quadratic maps.* Comm. Math. Phys. **146** (1992), 123-138.